Large Displacement Fast Conducting Polymer Actuators

by

Angela Ying Ju Chen

Submitted to the Department of Mechanical Engineering
in partial fulfillment of the requirements for the degree of

Master of Science in Mechanical Engineering

at the

MASSACHUSETTS INSTITUTE OF TECHNOLOGY

June 2006

Author .....
Department of Mechanical Engineering
May 12, 2006

Certified by .....
Ian W. Hunter
Professor
Thesis Supervisor

Accepted by .....
Lallit Anand
Chairman, Department Committee on Graduate Students

Large Displacement Fast Conducting Polymer Actuators

by

Angela Ying Ju Chen

Submitted to the Department of Mechanical Engineering
on May 12, 2006, in partial fulfillment of the
requirements for the degree of
Master of Science in Mechanical Engineering

Abstract

Conducting polymers are a promising class of electroactive materials that undergo volumetric changes under applied potentials, which make them particularly useful for many actuation applications. Polypyrrole , is one of the most common conducting polymers of choice for the development of actuator technologies and has been well characterized in its mechanical, electrical, and electrochemical response. Although capable of producing almost 10 times more active stress for a given cross-sectional area than skeletal muscle, strains are relatively low on the order of 1 to 2 %, as are strain rates, which are on the order of a couple percent per second. Small strains can be amplified to produce large bending displacements by configuring the conducting polymer film in a trilayer configuration with two conducting polymer films sandwiching an electrolyte gel layer.

This thesis focuses on the development of conducting polymer bending actuators in air. There is a strong correlation found between applied voltage, temperature, and the speed of actuation. Several experiments were carried out to determine the effect of temperature on the mechanical, electrical, and electrochemical properties of the components of the trilayer. This data coupled with thermal profiles of trilayers during actuation, electrochemical profiles, and force generation plots of the trilayers shed light on how these bending actuators can be optimized and integrated into different applications such as propulsion mechanisms for autonomous underwater vehicles.

Thesis Supervisor: Ian W. Hunter
Title: Professor

Acknowledgments

I would like to take this time to thank the many people who made this possible.

First and foremost, I would like to thank Professor Ian Hunter for his support and mentorship. I am constantly amazed by his depth and breath of knowledge, which he shares with his students. He has provided us with an environment filled with endless resources and possibilities that stimulate the mind and entice the imagination.

I am grateful for Patrick Anquetil for all of his guidance, encouraging words, and consistently positive outlook on life during my time as an undergraduate and graduate student. I would also like to thank him for proofreading a draft of my thesis. Thanks also to James Tangorra who helped to steer and motivate the entire MURI team to make sure we were always funded. My sincere gratitude goes out to Nate Vandesteeg, Rachel Pytel, Brian Hemond, and Bryan Ruddy for their expertise on various subject matters such as coding, electrochemistry, materials science, electronics, and experimental set-ups. I highly respect their opinions and input. They were an invaluable resource to have in the lab during these past two years. Thanks again to Nate for reading a draft of my thesis and helping me out with all of my thermal experiments. Special thanks to Mike Del Zio for always keeping things fun, interesting, and never too high strung in the lab. I am grateful for Naomi Davidson and Laura Proctor for their friendship and support. Thanks to Priam Pillai for his Matlab expertise and his ability to condense my pages of code into one line commands. Thanks to Tim Fofonoff for always being there for me to bounce ideas off of. Thanks go out to the rest of my colleagues in the BioInstrumentation Lab. It was an honor to have worked with and learned from all of them.

There are several people outside of the lab that I'd like to thank. Grad school would have been a lonely and boring place without them. Thanks to the Perfect Strangers. There are so many memories that I will cherish because of them: ski trips, camping trips, IM sports, barbecues, movies, nights out, and nights in. Their friendship has made these last two years a wonderful experience. To my roommates, you were so much fun to live with. Thanks for putting up with my turtles for the

past year and a half. To everyone else that I regularly interact with, thank you for your friendship and support.

Last but not least, I'd like to thank my family: my father, William; my mother Susan; and my brother Justin. They have stood by me throughout the years and offered their unwavering support in all that I have chosen to pursue. I am so grateful to have such a loving family.

Contents

List of Figures

List of Tables

Chapter 1

Introduction

Conducting polymers possess a wide range of properties that make them ideal for many different types of applications, one of which is actuation. Interest in conducting polymers as a viable actuator technology began in the early nineteen nineties [5]. Under electrochemical stimulation, conducting polymers exhibit volumetric changes during the oxidation and reduction processes. Typical strains seen in conducting polymer films is on the order of a few percent.

A common method of amplifying the strain is to assemble the conducting polymer into a bilayer or trilayer configuration to convert small linear strains into large bending motion. Several models have been developed to describe the behavior of these bending actuators. Pei and Inganas developed a model which predicted the displacement of bilayers [28], and Madden presented a model which predicted displacement of trilayers and force output from both bilayer and trilayer actuators [23]. These models served as invaluable tools for developing conducting polymer actuators for various engineering applications. Some of the applications that have been explored include manipulation and microrobotics ([13], [33], [26], [27]),biomedical devices ([34], [15], [9]), sensors, ([16])and control of hydrodynamic surfaces in underwater vehicles ([21], [22]).

While the theoretical capabilities of conducting polymers are very impressive, one of the challenges that is often encountered and prevents the polymers from being readily incorporated into many applications is the relatively slow speed of actuation observed due to the fact that the strain rate is diffusion limited. Recent studies

focused on improving the strain rate by applying a shaped voltage potential. Strain rates of up to 3 $\%s^{-1}$ were generated with power to mass ratios comparable to skeletal muscle ([20], [12]). Madden showed that high applied potentials led to increased strain rate and power to mass ratios in conducting polymer actuators. Degradation could be avoided by limited the amount of time that the potentials were applied to the polymer [20].

This thesis focuses on the improving the trilayer actuator in terms of speed of actuation and force production so it can be a viable actuator in applications such as autonomous underwater vehicle propulsion. The method of increasing applied potential suggested by Madden was employed to achieve fast actuation. Although, the specific shaped potential that was created via a feedback loop was not used. An effect observed from applying these overpotentials was an increase in temperature of the trilayer and a subsequent increase in strain rate. Studies were done to further understand the effect that heating had on trilayer performance.

Short sections in the remainder of this introduction cover some of the background on the specific conducting polymer used for actuator development, the mechanism by which it undergoes volumetric changes, and more specifically, the trilayer actuator which converts these small volumetric changes into large bending motions.

1.1 Polypyrrole Background

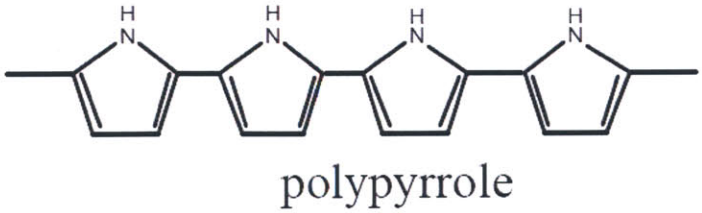

polypyrrole

Figure 1-1: Molecular structure of polypyrrole.

Polypyrrole (Figure 1-1) is the conducting polymer of choice for actuator development discussed in this thesis . Out of many the conducting polymers such as polyaniline, polythiophene, polyphenylene, and polyacetylene, polypyrrole is the

most robust. Current electrochemical synthesis techniques repeatedly produce relatively large quantities of polypyrrole with stable electrical and mechanical properties. Many studies have been done to characterize polypyrrole, and several models have been developed to predict its mechanical response. Polypyrrole can generate active stresses as high as 40 MPa ([18]) and exhibit maximum strains on the order of 10 to 26% ([2],[6],[18], [11]). In general, typical values for actuators range from 1 to 2% strain with active stresses of about 5 to 10 MPa. Typical conductivities of polypyrrole are on the order of 10^4 Sm^{-1}. While there is still room for discovery in terms of understanding polypyrrole as an engineering material, it has proven to be the most reliable conducting polymer to use in various actuation applications. In its neutral state, polypyrrole is an insulating material. However, the polymer can be electrochemically "doped" to transform it into a conductive state. Figure 1-2 details the mechanism of polypyrrole polymerization during the "doping" process. Polypyrrole is able to conduct because of its conjugated backbone meaning single and double bonds alternate along the polymer chain (Figure 1-1). Polypyrrole conducts via electron delocalization along the length of the polymer chains as voltages are applied ([17], [30], [4]). Once an electron is introduced to convert a double bond into a single bond, the next bond is forced to convert from a single bond to a double bond. This effect propagates along the polymer chain to maintain the conjugated structure. Therefore, conductivity of the polymer is heavily dependent on the structure of the polymer and the orientation of the polymer chains within the material. It is most conductive along the length of the chain, and less conductive across different chains. Even though polypyrrole chains are anisotropic in nature, synthesis of polypyrrole results in many polypyrrole chains that are randomly oriented. Without any post-processing of the material, the result is a sheet of polypyrrole that is isotropic in its electrical and mechanical properties.

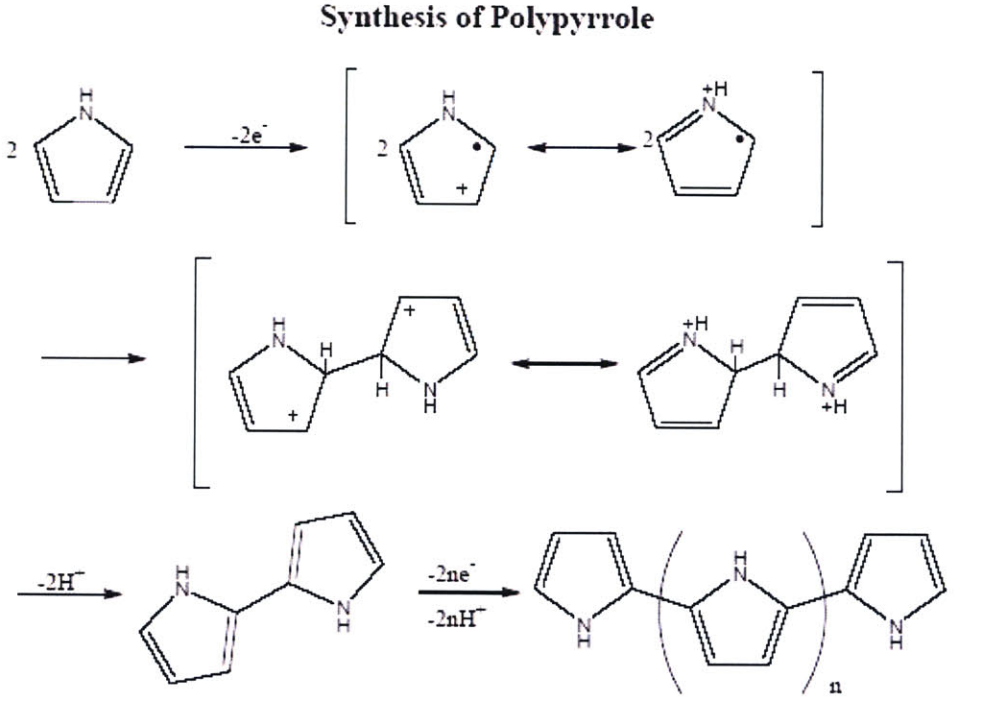

The last step is a in fact a repetion of the first steps beginning with oxidation, followed by coupling to either end of the polymer, and finally elimination of H^+. The electrons are either removed via an electrode (electrochemical deposition) or chemically, e.g.

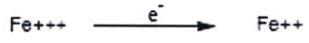

Note that the polymerization does not generally result in a neutral polymer shown above, but rather the backbone is charged, as below, such that the total number of electrons transferred per monomer is $2-a$ where a is generally between 0.2 and 0.5:

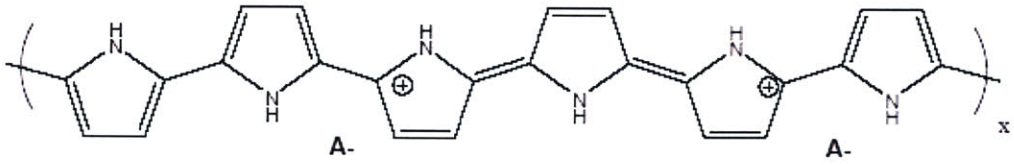

where A^- is an anion or dopant. Here a=1/3. During the initial phases of electrodeposition the oligomers remain in solution, eventually precipitating to form a solid with intercalated anions.

Figure 1-2: Mechanism of polypyrrole polymerization. Source: [17].

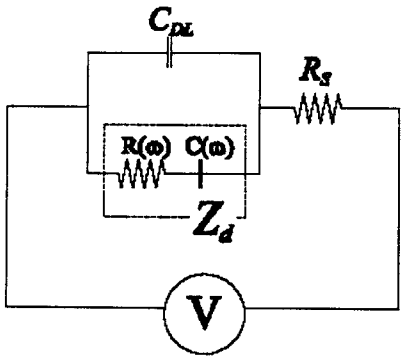

Figure 1-3: Circuit model of a conducting polymer in the presence of an electrolyte. Source: [23].

1.2 Polypyrrole actuation

Conducting polymer actuation can be described using a diffusive elastic model first developed and derived by John Madden in his Ph.D thesis [17]. The model describes the electrical and mechanical behavior of a thin strip of polypyrrole placed in an electrolyte solution with a counter electrode present to control applied voltage [1]. The equivalent circuit model of the polymer in electrolyte is shown in Figure 1-3 where R_s is the series resistance which includes the resistance of the electrolyte solution and any contact resistance, C_{DL} is the double layer capacitance, and Z_D is the diffusion impedance which includes a bulk capacitance term. The charging of the bulk capacitance of the polymer contributes to the volumetric expansion and contration of the polymer.

Qualitatively, the mechanism by which polypyrrole expands or contracts is depicted in Figure 1-4. As a voltage is applied across the electrolyte between the strip of polypyrrole and the counter electrode, the polypyrrole becomes either positively or negatively charged. Ions from the electrolyte diffuse into the bulk of the polymer to balance the charge. Diffusion of ions into the polymer results in expansion while diffusion of ions out of the polymer results in contraction. If both positive and negative ions are able to diffuse into and out of the polymer, the expansion due to

[1]Refer to [19] or chapter 2 of [23] for a condensed overview of the empirically and physically based models describing electrochemical actuation of hexafluorophosphate-doped polypyrrole

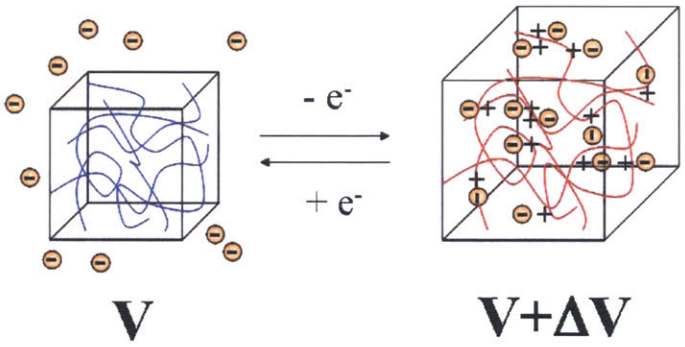

Figure 1-4: Schematic representation of the volume change that occurs during the electrochemical switching of polypyrrole. Source: [24].

the movement of one ion is counteracted by the contraction due to the movement of the oppositely charged ion [28] However, by choosing an electrolyte where one ion is much larger than the other, the flux into and out of the polymer is dominated by the smaller ion since the large ion is rendered immobile due to it's size.

Figure 1-5 shows the charging behavior of the polymer over time as a voltage is applied. If the polymer is reduced, positive ions are attracted to the surface of the polymer and negative ions are repelled. If the polymer is oxidized, positive ions are repelled and negative ions are repelled. Initially, the movement of ions does not contribute to the expansion or contraction of the polymer. Instead, it contributes only to the charging of the double layer at the interface of the polymer and the electrolyte. Once the double layer is charged, the concentration gradient drives diffusion of the ions into or out of the polymer resulting in a volumetric change.

According to Madden [19], There are three primary rate limiting constants. These time constants are important in assessing polymer actuator performance. τ_{RC} is the time constant that describes the charging time of the double layer. τ_{DDL} is the time constant that describes the diffusion of ions through the double layer thickness. τ_D is the time constant that describes the diffusion of ions into the polymer. These time constants should be minimized to maximize actuator performance.

$$\tau_D = \frac{h^2}{4 \cdot D}, \tag{1.1}$$

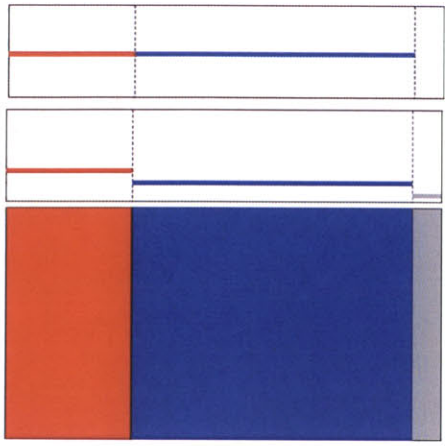

(a) The polymer at rest. There is a voltage difference at the interface between the polymer and the electrolyte and at the interface between the electrolyte and the counter electrode.

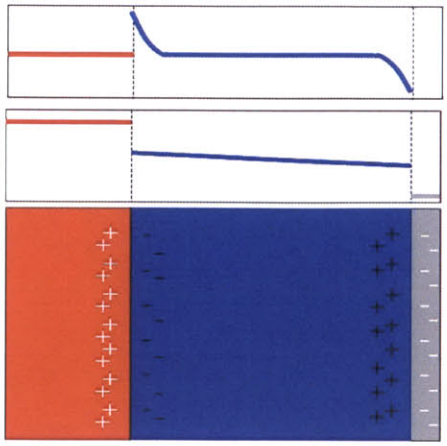

(b) When a potential is applied, a current begins to flow through the electrolyte and ionic charge builds up in the double layers.

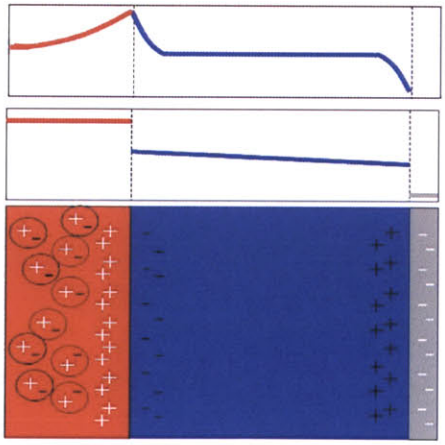

(c) The concentration of ions at the polymer surface drives the diffusion of ions into the polymer. Inside the polymer, the ions are paired with holes or electrons to form neutral species.

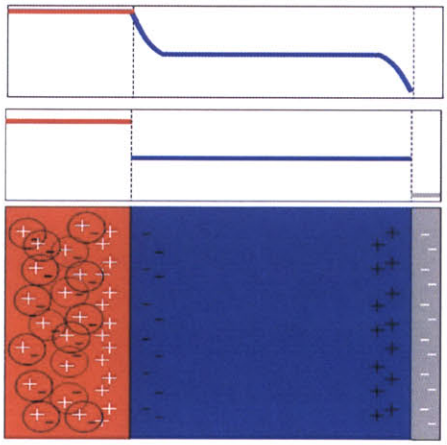

(d) The polymer if fully charged when the concentration of ions in the polymer is equal to the concentration of ions in the double layer at the polymer electrolyte interface.

Figure 1-5: Charging of the conducting polymer. The upper two plots of each figure show the ion concentration and the voltage in the polymer (polypyrrole, red), in the electrolyte (blue), and the in the counter electrode (gray). The figure depicts charging for single ion (anion) movement into and out of the polymer. Source: [23].

$$\tau_{RC} = R \cdot C_{dl} = \frac{d}{\sigma_e \cdot A}, \tag{1.2}$$

$$\tau_{DDL} = \frac{\delta^2}{D}, \tag{1.3}$$

where

h - Thickness of polymer strip

D - Diffusion coefficient of the ion within the polymer

R - Series resistance including electrolyte and contact resistances

C_{dl} - Double layer capacitance

d - Separation between the film and the counter electrode

σ_e - Conductivity of the electrolyte

A - Surface area of the polymer film

δ - Thickness of the double layer

From these equations, one can extract the important variables that should be adjusted for optimal performance. Variables to be minimized are thickness of film h, distance between electrodes d, series resistance R, double layer capacitance C_{dl}, and double layer thickness δ. Variables to be maximized are ion diffusion coefficient D, electrolyte conductivity σ_e, and surface area of the film A.

Peter Madden related the time constants from the diffusive elastic model to physical material properties of the polymer and the electrolyte [23]. The most relevant material properties that affected or were affected by the temperature studies done in this thesis were degradation voltage, electrolyte resistance, and polymer resistance. The degradation voltage is a practical limit on the peak concentrations of ions in the double layer. The maximum ion concentration sets the maximum ion diffusion rate, and thus the maximum stress and strain rates. Electrolyte resistance affects the double layer charging time. Reducing the electrolyte resistance results in faster charging of the double layer. Polymer resistance creates a voltage drop along the length of the polymer. Energy is lost through resistive heating and the voltage drop

results in a decrease in ion concentration and thus slower actuation in areas of the polymer farther away from the current source.

1.3 Bending actuators

Figure 1-6: Components of a trilayer. Two polypyrrole films ($\approx 20\ \mu m$) sandwich an ion permeable membrane with electrolyte gel ($\approx 75\ \mu m$). Total thickness of a typical trilayer is $115\ \mu m$.

Conducting polymers are often operated linearly in a liquid electrolyte bath. However, typical strains observed range from 1 to 2%. A trilayer configuration can be used to amplify the small strains. Figure 1-6 shows the typical dimensions of a trilayer. In the trilayer, the middle layer is in inactive layer composed of ionically conducting gel, while the outer two layers are conducting polymer strips which compliment each other with expansion and contraction converting small linear changes into large deflections (Figure 1-7). One advantage of the trilayer configuration is that it removes the need for a liquid electrolyte bath, thus making a nice actuator package that can be operate in air.

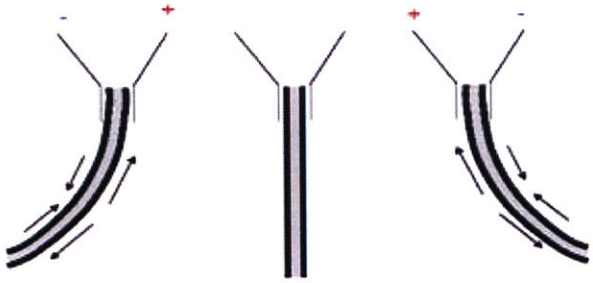

Figure 1-7: Method by which a trilayer actuates.

The conducting polymer layers in a trilayer expand and contract according to the diffusive elastic model described earlier. Figure 1-7 illustrates the method by

which a trilayer actuates. Initially, positive and negative ions from the electrolyte are dispersed evenly throughout the entire trilayer. The conducting polymer layers act as ion reservoirs. As voltage is applied across the layers of polypyrrole, one side is oxidized while the other side is reduced. An electrolyte is chosen so that one ion is larger than the other. In this case, the cation is rendered immobile due to its size, while the anions flow out of the negatively charged layer causing contraction, and into the positively charged layer causing expansion. When the voltage is reversed, the same anion movement occurs but in the other direction.

1.3.1 Modeling of Bending Actuation

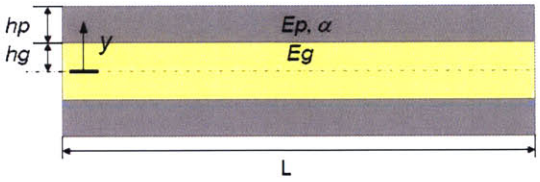

Figure 1-8: Geometry of a trilayer.

Equations that relate the deflection of trilayers and force generation to the geometry and expansion of the conducting polymer layers were derived by Madden and Schmid [23],[31]. The trilayer is modeled as a composite beam with top and bottom layer consisting of conducting polymer and the middle layer consisting of ionically conducting gel (Figure 1-8).

Assuming uniform curvature along the trilayer, the strain is given by:

$$\epsilon(y) = K \cdot y\,, \tag{1.4}$$

where ϵ is the strain, K is the curvature of the trilayer, and y is the distance from the center line of the trilayer. Internal stresses experienced by the polymer and the electrolyte gel are given by:

$$\sigma_g(y) = E_g \cdot \epsilon_g(y)\,, \tag{1.5}$$

and

$$\sigma_p(y) = E_p \cdot (\epsilon_p(y) + \alpha \cdot \rho)\,, \tag{1.6}$$

where E_g and E_p are the elastic modulus of the polymer and electrolyte gel, ϵ_g and ϵ_p are the local strain of the polymer and gel, α is the strain to charge ratio, and ρ is the charge density in the polymer.

The curvature produced by an internal bending moment induced by the stress in the polypyrrole is ultimately dependent on the stiffness of the trilayer structure. The flexural rigidity of the trilayer is given by the equation

$$EI = E_p I_p + E_g I_g\,, \tag{1.7}$$

where I is the area moment of inertia for the strips of polypyrrole and the layer of electrolyte gel.

Balancing the all the moments present in the system results in a relationship between force, curvature, and charge density. In the case of free deflection, the curvature to charge density ratio is

$$\frac{K}{\rho} = -\frac{3\alpha}{2h_g}\left[\frac{\left(1+\frac{h_p}{h_g}\right)^2 - 1}{\left(1+\frac{h_p}{h_g}\right)^3 + \left(\frac{E_g}{E_p} - 1\right)}\right]. \tag{1.8}$$

In the case of zero deflection, the force to charge density ratio is

$$\frac{F}{\rho} = \frac{E_p \alpha}{2h_g} W h_g^2 \left[\left(1+\frac{h_p}{h_g}\right)^2 - 1\right]. \tag{1.9}$$

These equations serve as useful tools for the design of trilayer actuators with specific deflection and force requirements.

1.4 Chapter descriptions

Chapter 2

The fabrication process of the trilayer actuators studied is detailed in this chapter. Electrochemical deposition of the polypyrrole is discussed as well as methods to inspect the quality of films produced. Method of making the electrolyte gel is covered, and trilayer assembly techniques are explained.

Chapter 3

Observations of trilayer heating during actuation is summarized in this chapter. Temperature profiles of trilayers activated under various actuation schemes were generated via image processing of thermal video data. Different methods of electrical contact placement including single ended and double ended contacts were explored.

Chapter 4

Experiments performed to determine the effect of heating on the different components of the trilayer are discussed. Results show the effect of temperature on the mechanical, electrical, and electrochemical properties of the electrolyte gel and the polymer.

Chapter 5

Force generation graphs of trilayers actuated under different conditions are presented. Trilayer performance is shown to depend heavily on the impedance, or series resistance, of the trilayer. A duty cycle actuation scheme is presented to overcome series resistance issues in the electrolyte gel. Artifical heating is introduced to decrease series resistance.

Chapter 6

Conducting polymer actuators have a lot of potential in the field of autonomous underwater vehicle propulsion. This chapter describes steps that have been taken to

integrate conducting polymers into a biomimetic pectoral fish fin for maneuvering in hydrodynamic applications.

Chapter 7

This chapter gives a quick summary of the work covered in this thesis.

Chapter 2

Fabricating Trilayers

Trilayer performance depends heavily on the quality of polypyrrole films and electrolyte gel being used. In the following sections, the method of making the polypyrrole film and electrolyte gel, the main components of a trilayer will be discussed followed by an explanation of the trilayer construction process.

2.1 Polypyrrole Film

2.1.1 Deposition Technique

The polypyrrole film that is used to assemble the trilayers is manufactured via an electrochemical deposition process. The deposition solution used consists of 0.05 M distilled pyrrole monomer and 0.05 M tetraethylammoniumhexafluorophosphate in propylene carbonate with 1% distilled water. First, the propylene carbonate, tetraethylammoniumhexafluorophosphate, and distilled water are mixed thoroughly. This solution can be stored as stock solution. The distilled pyrrole is not added until immediately before the start of a deposition to minimize the amount of time that it is exposed to the outside environment. Overexposure to air will cause the pyrrole to oxidize and degrade resulting in low quality films. Once the pyrrole is added, nitrogen is bubbled through the solution for 10 to 15 minutes. The nitrogen is denser than air and sinks down to provide a protective layer between the pyrrole and the outside

enviroment.

Polypyrrole films are grown on a glassy carbon crucible (Figure 2-1), which serves as the working electrode. Crucible cleaning and preparation is further detailed in

Figure 2-1: Polypyrrole film deposited on a glassy carbon crucible.

Brian Schmid's thesis [31]. Copper shim stock is placed around the crucible to serve as the counter electrode. The deposition solution is poured into a beaker with the crucible and copper sheet and placed in a MicroClimate Chamber which is set to -40 °C. To ensure best results a thermocouple is placed in the deposition solution, and the deposition is not started until the solution temperature has reached -40 °C.

The deposition can begin once the solution is cooled down to the desired temperature. A VMP Multichannel Potentiostat [1] is used to run the electrochemistry. Currently, depositions are performed galvanostatically at $0.5\frac{A}{m^2}$ for 10 hours which result in 15 to 20 μm thick films. The desired thickness of films can be set by adjusting the duration of the deposition.

Once a deposition has finished, the carbon crucible is removed from the deposition solution. The film is rinsed with the stock deposition solution, without the pyrrole added, to remove any debris or pyrrole monomer left on the surface of the film. The film is allowed to dry on the crucible under a fume hood for 6 to 12 hours to allow the solvent to evaporate. After most of the solvent has evaporated, the polypyrrole film can be easily peeled off the crucible.

[1] Princeton Applied Research, www.princetonappliedresearch.com

Polypyrrole films are stored in polyethylene bags until they are needed for mechanical testing or trilayer fabrication. For best actuation properties, it is best to use freshly deposited polypyrrole films. There is an aging effect in the material properties of polypyrrole. Over time, the film loses its elasticity and exhibits poorer performance in actuation.

2.1.2 Quality Inspection

It is important to be able to visually inspect a film to gauge its quality. In general, polypyrrole films that actuate well are easy to peel off from the crucible, they lay flat once they are removed, and they have a consistent texture and black color on both the solution side and crucible side of the film. In contrast, polypyrrole films that exhibit lower actuation performance do not not peel off the crucible easily , they tend to curl up on themselves, and the solution side of the film usually exhibits areas of brownish discoloration and has more of a glossy texture.

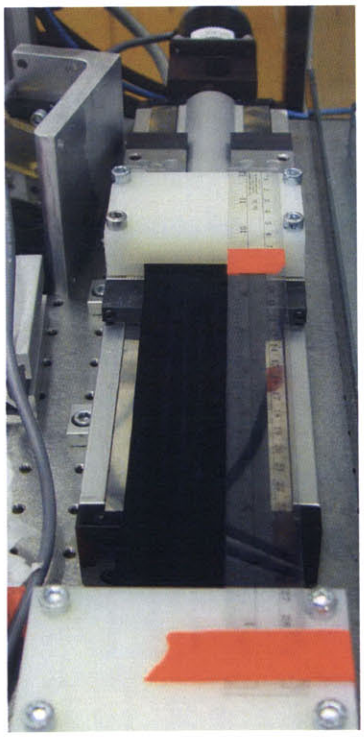

Figure 2-2: Stretcher used to test film elasticity.

Another method to predict the assess the quality of a film as an actuator is to test its elasticity. Figure 2-2 shows a stretching device used for this purpose. One clamp is fixed while another clamp is mounted on a linear stage. Its position can be adjusted manually by turning a knob on the end of the stage. The polypyrrole film that will be used for actuation is clamped at two ends. The position of the clamp is adjusted to eliminate any slack in the film. A small dynamic strain ($\approx 5\%$) is applied to the film. Cyclically stretching the film by hand is a good way to get a sense of the compliance of the film. Polypyrrole films that actuate well tend to be slightly more compliant than films that do not. Poor quality films have a higher Young's Modulus and reach their break point after experiencing smaller strains. Trilayers constructed with stretched films exhibited a preferential direction of curl around the axis perpendicular to the direction of stretch. It is not fully understood how cyclically stretching the polypyrrole at a low dynamic strain affects the polymer chain alignment and morphology. However studies have shown that highly stretched polypyrrole films do exihibit anisotropy in conductivity and electroactive strain [29].

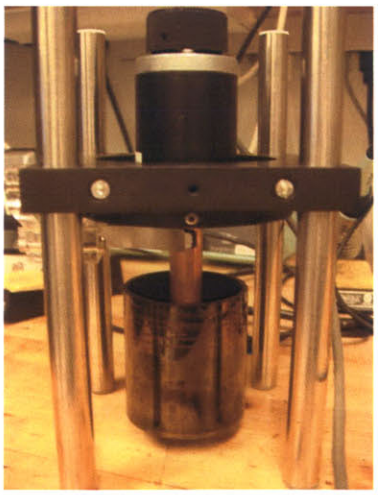

(a) Rotating glassy carbon electrode mounted to stepper motor.

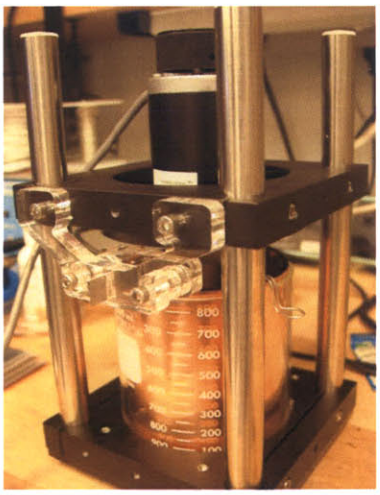

(b) Complete rotating deposition chamber.

Figure 2-3: Rotating deposition chamber used for producing uniform films.

In some cases, striation patterns form on the surface of the deposited polypyr-

role. This usually indicates the presence of excess moisture in the environment. Water condenses and freezes on the deposition container and drips into the deposition solution resulting in a solution with nonuniform concentrations of pyrrole. These non-uniformities result in the striated pattern where less pyrrole is being deposited. The fingering phenomenon does not occur very often when depositions are done in a controlled environment. However, in cases where a carefully controlled, low moisture environment cannot be avoided, it is helpful to place a lid on the deposition container to prevent large ice crystals from dropping into the solution. Another method to avoid the fingering pattern on the film is to keep the deposition solution constantly mixed. A rotating deposition chamber was built for this purpose (Figure 2-3). The glassy carbon crucible is rotated by a stepper motor at a constant speed which keeps the deposition solution constantly mixed.

2.1.3 Surface Morphology of Films

One of the factors that seems to have an affect on the performance of polypyrrole films, is the surface morphology of the film. Figure 2-4 shows SEM images taken of two different polypyrrole films with distinct surface morphologies. The images on the top capture the face on view of the crucible side of the film. The images on the bottom capture an area of the polypyrrole film that is folded over so that both crucible and solution sides of the film are visible. The surface of the film shown in Figure 2-4(a) is completely flat. There are no defining characteristics on either side of the film. In contrast to the flat film, Figure 2-4(b) shows a film that has evenly distributed pores that range in size from 10 to 25 μm in diameter over the crucible side of the film. Corresponding bumps of the same size are present on the solution side of the film, which suggest that bubbles are forming on the surface of the crucible as polypyrrole is being deposited. The porous films have a larger surface area for ion exchange and diffusion. It is not known what causes the bubbles to form on the surface of the film although other studies have made similar observations in surface morphology [7]. For comparison, both films were used to manufacture trilayers, which were then actuated with a ± 9 V signal to compared performance. The trilayers made with the porous

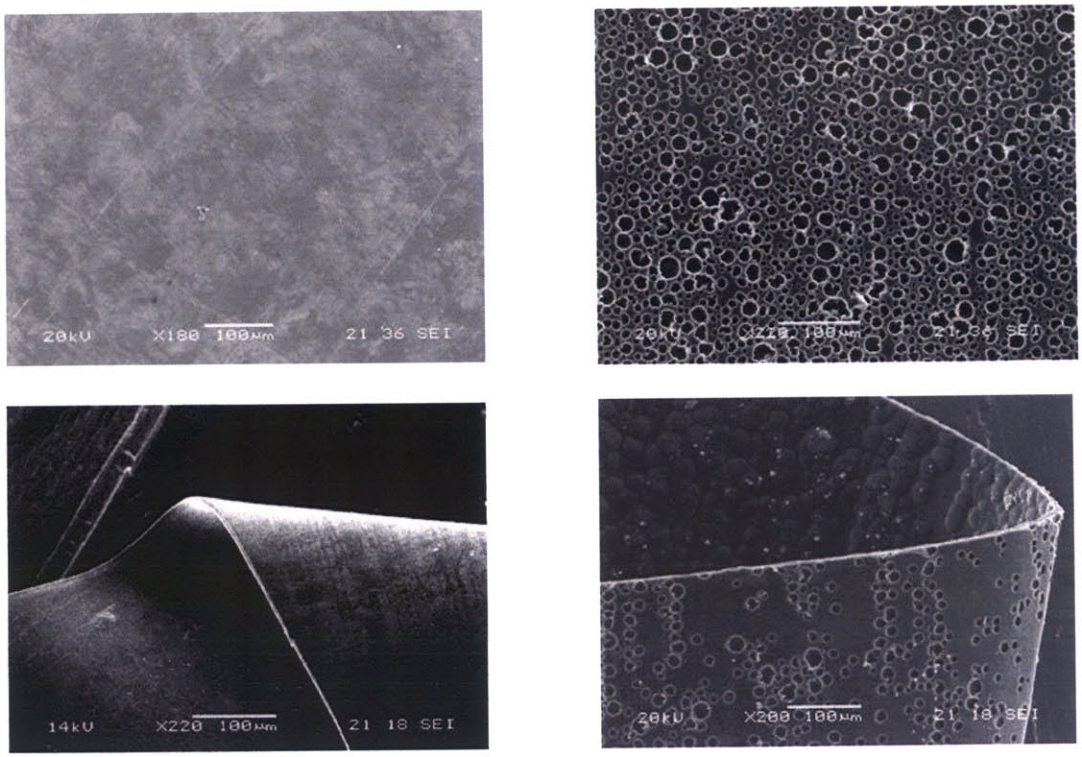

(a) Flat morphology

(b) Porous morphology

Figure 2-4: Two polypyrrole films with distinct surface morphologies.

films exhibited a markedly faster response achieving full sweeps at about 2 Hz, while the trilayers made with the flat films were much slower and actuated at frequencies closer to 0.25 Hz.

2.2 Electrolyte Gel

In order for polypyrrole to undergo a volumetric change, there must be a source of ions. In linear actuation, polypyrrole is usually actuated in a liquid electrolyte bath with a separate counter electrode. For actuation in air, as in the case of the trilayers, the liquid electrolyte is suspended in a gel medium. In addition to serving as the ion source, the electrolyte gel also serves as an adhesive to hold the two layers of polypyrrole together since one layer needs to act as the counter electrode for the other. Table 2.1 shows the recipe that is used to prepare the electrolyte. Liquid

Ingredients	Molarity%	Desired Mass(g)
Liquid Salt $BMIMBF_4$ (226.03 g/mol)	40%	10.00
2-Hydroxyethyl methacrylate (130.14 g/mol)	58.4%	8.41
Ethylene glycol dimethacrylate (198.22 g/mol)	0.8%	0.175
Azobisisobutyronitrile (164.21 g/mol)	0.8%	0.145

Table 2.1: Electrolyte Gel Composition.

(a) Six month old electrolyte gel.

(b) Freshly mixed electrolyte gel.

Figure 2-5: Electrolyte gels stored for different amounts of time and cured at 85 °C for 20 minutes. Gels exhibit crystal patterns and areas of phase separation. Images are taken at 2× magnification.

salt 1-Butyl-3-methyl-imidazolium tetrafluoroborate, or $BMIMBF_4$, is the electrolyte. Methacrylate is the gel polymer that is crosslinked to form a gel. Dimethacrylate is the cross-linking agent, and Azobisisobutyronitrile is the initiator that begins the crosslinking process. The electrolyte gel mixture is stored thoroughly mixed and stored in a freezer at -20 °C to prevent or slow down any premature crosslinking in the gel. Over time the electrolyte gel will continue to crosslink to a point where trilayer performance is noticeably decreased. Figure 2-5 shows the difference between freshly mixed electrolyte gel and electrolyte gel that has been stored for six months. Samples were cured at 85 °C for 20 minutes. Both gels have interesting crystal patterns and areas of phase separation between the liquid salt and the gel dispersed throughout. However, the patterns are larger and more dense in the gel that has been stored for almost six months (Figure 2-5(a)).

2.3 Trilayer Construction

Polypyrrole films used to construct trilayers are first inspected for quality as discussed in Section 2.1.2. Two sheets of polypyrrole are cut to size. The exact dimensions are not critical, since trilayers can be cut to the desired size and shape afterwards. One layer of polypyrrole is placed on a Teflon sheet with the crucible side of the polymer facing up. Next, two sheets of Kodak lens cleaning paper are laid on top of the first layer of conducting polymer. The Kodak lens cleaning paper is used as an ion permeable separator since the two conducting polymer layers must be electrically isolated from each other. The number of layers used can be changed. The thickness of the middle layer of the trilayer affects the extent of the resulting curvature and the amount of force it can produce. Increasing the thickness of the middle layer results in a stiffer trilayer, which can exert more force. However, the greater force comes at a sacrifice of the rate of change of curvature [31]. Electrolyte gel is carefully applied and allowed to soak through the lens paper. The final layer of polypyrrole is laid on top of the electrolyte soaked lens paper with the crucible side of the film facing down. Another Teflon sheet is placed on the trilayer structure. The assembly is clamped between two plates and placed in an oven set at 85 °C. The electrolyte gel takes less than 20 minutes to cure. The polypyrrole shrinks during the heating process eliminating any initial wrinkling in the film. The trilayer can be removed and is ready to use after an hour or two in the oven. However, it is best to store the trilayer in the oven until it is ready to be used. Trilayers fresh out of the oven actuate much faster than trilayers that have been stored at room temperature. Later discussion will reveal why this behavior may occur. For a typical trilayer, the thickness of the polypyrrole film is 20 μm and the electrolyte gel layer with the ion permeable membrane is 75 μm resulting in a total thickness of 115 μm.

2.4 Summary

The trilayer fabrication process includes depositing the conducting polymer film, mixing the electrolyte gel, assembling the trilayer package, and baking the trilayers to cure the electrolyte gel. The polypyrrole and electrolyte gel mixture should be tested regularly for quality to ensure the best performance. Once baked, trilayers can be cut to any shape or size to be used in experiments (Chapter 3 and 5) or other applications (Chapter 6).

Chapter 3

Trilayer Heating

In many studies, trilayer actuation has been limited to small voltage ranges on the order of 1 volt to achieve uniform curvatures. However, in many applications, it is not the curvature that is important, but the speed of actuation. John Madden showed that strain rates in polypyrrole actuation could be improved by increasing applied potentials [20]. Therefore, in many of the tests that were carried out in this thesis, trilayers were actuated in the operating range of 3 to 12 volts to maximize actuation speed while avoiding degradation. Because of the high voltages used to actuate the trilayers and the low efficiencies that trilayer exhibit for electrical to mechanical conversion [17], joule heating becomes a big factor which affects actuation. This chapter discusses the observations made on trilayer heating during actuation.

During trilayer actuation, it was observed that at initial applied voltage cycles, trilayer actuation started off relatively slow. As subsequent voltage cycles were applied, actuation speed increased. To better understand what caused this increase in speed, a Thermovision A40 Infrared Camera [1] was used to study the thermal behavior of the trilayer during actuation.

Another observation made during actuation was that at the higher voltages, trilayers did not exhibit uniform curvature along the length. Instead, the curvature was restricted to the area near the electrical contacts. Only a short length of the film at the base of the trilayer contracted. Under the thermal camera, this area could be

[1] FLIR Systems, www.flirthermography.com

polymer, Z_p, and the in plane electrochemical impedance of the the electrolyte in the ion membrane,Z_e. According to Equation 1.8, The curvature induced by the bending moment in a trilayer is proportional to current density. For constant curvature along a trilayer, the following condition must be met

$$Z_e >> Z_p . \tag{3.1}$$

If, on the other hand

$$Z_e << Z_p , \tag{3.2}$$

the current density along the polymer becomes concentrated at the base of the trilayer causing localized actuation.

3.2 Heat Equation

Localized heating also occurs in the areas of actuation. The ratio of impedances of the polymer and the electrolyte determines how far current will flow down the length of the polypyrrole before it is balanced by the flow of ions in the electrolyte. The power consumed by a trilayer contributes either to the work required for the volumetric expansion and contraction of the polypyrrole, or it is lost through resistive heating. In the case where the motion of the trilayer is restricted, none of the power consumed contributes to mechanical work. Instead, it is all converted to heat. The heat generated is proportional to the square of the current, I, flowing through the polpyrrole and is described by

$$P = I^2 R . \tag{3.3}$$

Heat propagates down the length of the trilayer due to a thermal gradient. The rate of change of temperature can be described according to the heat diffusion equation

identified as the area of localized heating ocurring near the electrical contacts 3-1.

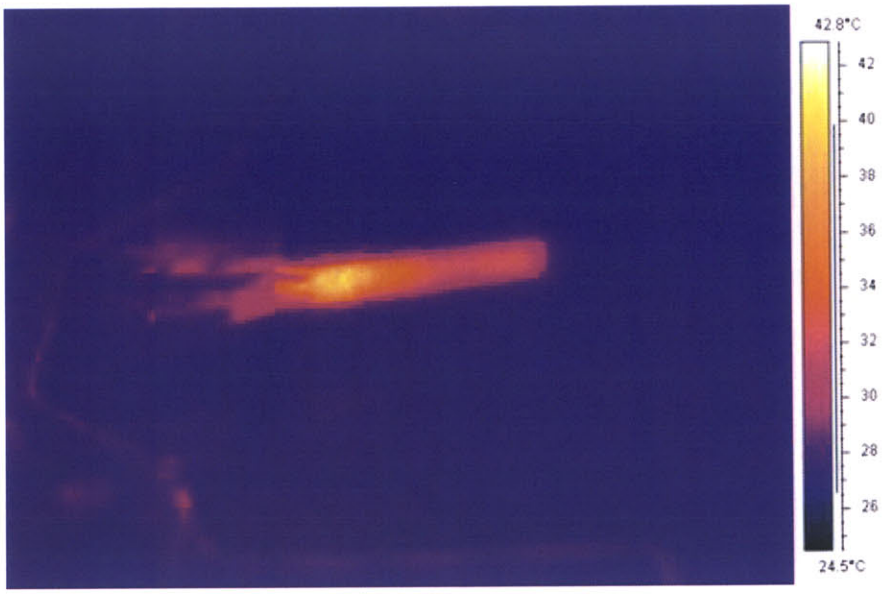

Figure 3-1: Localized heating taking place at the base of the trilayer near the electrical contacts.

3.1 Voltage Drop

The presence of localized heating indicates a large voltage drop across the polymer. Many models used to describe bending actuation assume uniform electrical potential along the length of the polymer. However, Peter Madden experimentally showed that this was not the case in [23]. Figure 3-2 shows the voltage profile versus position and time for both a low resistance and high resistance strip [2].

According to Peter Madden, polymer resistance affects the double layer charging rate, which in turn affects the the strain rate of polypyrrole. A voltage drop along the length of the polymer decreases the concentration of ions at the interface between the polymer and the electrolyte. The lower concentration gradient slows down the rate at which ions flow in an out of the polypyrrole.

Sherrit and Bar-Cohen also address the issue of local bending in ionic bender actuators [32]. They describe it in terms of ratio between the electrical resistance of the

[2]Experimental details can be found in Madden's thesis [23]

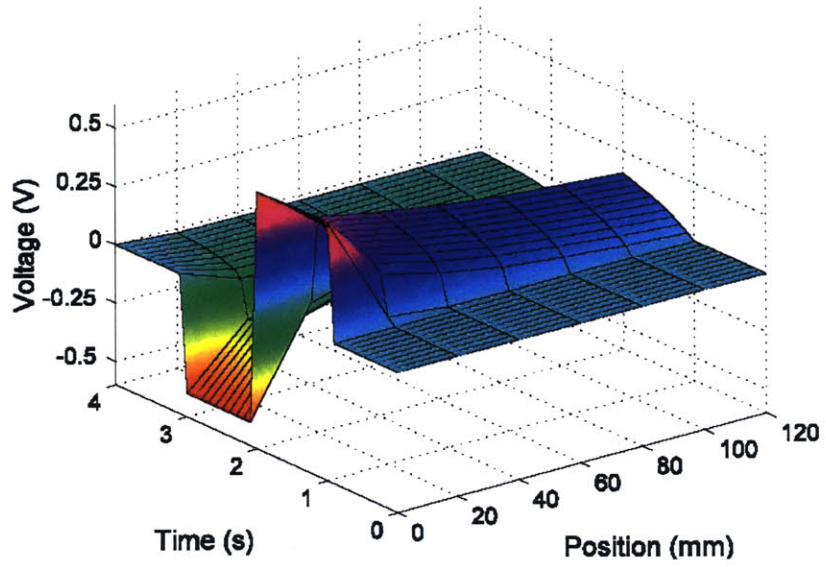

(a) High resistance strip of polypyrrole.

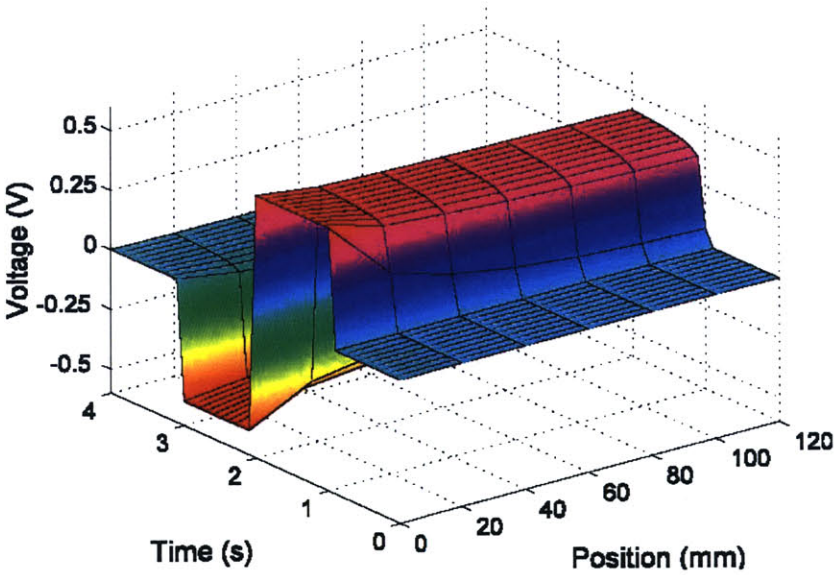

(b) Low resistance strip of polypyrrole.

Figure 3-2: Voltage versus position and time for polypyrrole strip of different resistances. Source: [23].

$$\frac{\partial T}{\partial t} = k\left(\frac{\partial^2 T}{\partial x^2} + \frac{\partial^2 T}{\partial y^2} + \frac{\partial^2 T}{\partial z^2}\right), \tag{3.4}$$

where T is the temperature as a function of time and space and k is material specific heat diffusion constant dependent the thermal conductivity, the density, and the heat capacity. For simplicity, the trilayer can be treated as one composite material instead of three layers of different materials.

Assuming the trilayer is much longer than it is wide, and since the thickness is very small, the equation can be simplified to the one dimensional diffusion equation

$$\frac{\partial T}{\partial t} = k\frac{\partial^2 T}{\partial x^2}, \tag{3.5}$$

where x is the direction along the length of the trilayer.

The trilayer has a capacity to store some of the heat generated via joule heating. The change in internal energy, e, is related to the trilayer's ability to store heat and can be described by the equation,

$$\frac{de}{dt} = \rho c\frac{dT}{dt}, \tag{3.6}$$

where ρ is the bulk density of the trilayer and c is the specific heat capacity of the trilayer. Following the principles of conservation of energy, the heat conducted out equals the heat generated from current flow minus the change in internal energy of the trilayer. The work term is ignored because the motion of the trilayer is restricted. The result is the well known one-dimensional heat diffusion equation with a current source term.

$$\frac{\partial T}{\partial t} - \frac{k}{\rho c}\cdot\frac{\partial^2 T}{\partial x^2} = I^2 R. \tag{3.7}$$

3.3 Temperature Measurements

The Thermovision A40 Infrared Camera was used to capture the spatial and temporal temperature profile of a trilayer during actuation. The dimensions of the trilayers used

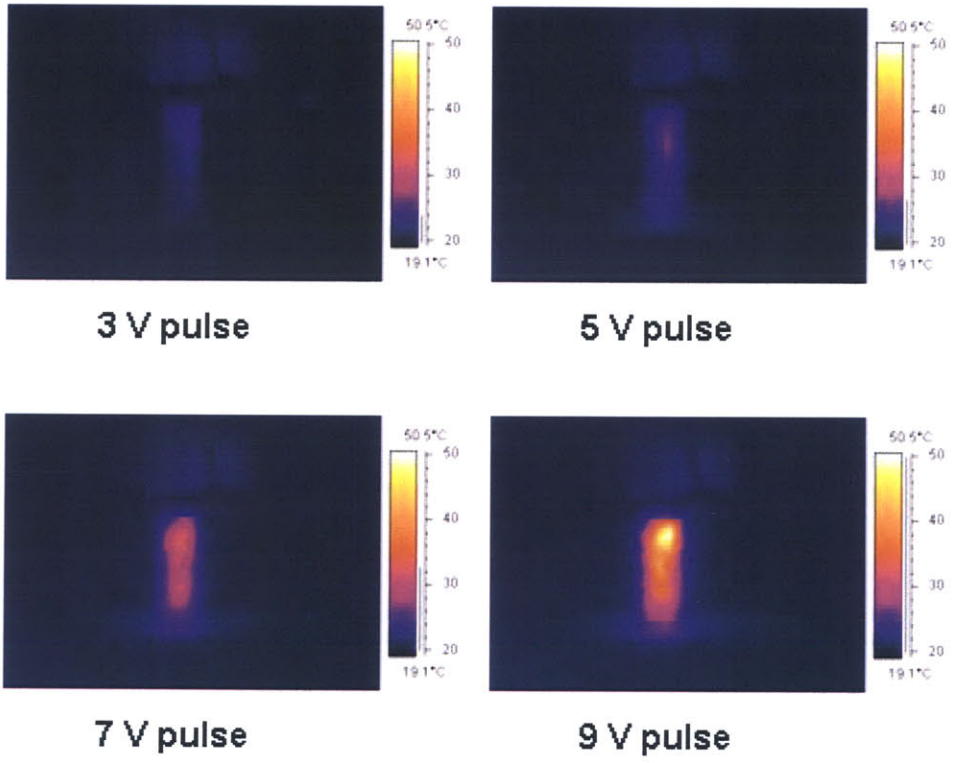

Figure 3-3: Images from the Thermovision infrared camera taken at the end of a 5 second pulse of 3, 5, 7, and 9 Volts.

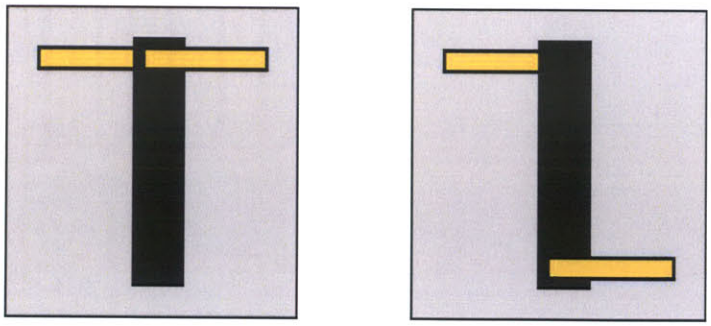

(a) Single ended electrical contact.

(b) Double ended electrical contact.

Figure 3-4: Schematics of two methods of electrical contact placement (orange) on the trilayer (black).

were 10 mm wide and 30 mm long. Trilayers were constrained from all sides to prevent actuation. Copper tape was clamped on either side to provide electrical contact to the trilayer (Figure 3-4(a)). A mounting block constructed out of foam was used to minimized heat loss through conduction between the surface of the trilayer and the mounting block. Several voltage controlled actuation schemes at various magnitudes and frequencies were explored to understand the heating and cooling behavior of the trilayer.

Electrochemistry was controlled and recorded by the VMP2 Multichannel Potentiostat[3]. Images such as the ones seen in Figure 3-3 were captured by the Thermovision infrared camera at a rate of 15 frames per second with a resolution of 320 by 240 pixels. For data analysis, everything but the area of the image containing the trilayer was cropped out. Temperature data was stored for each pixel in the saved area, and this process was repeated for every fifth frame resulting in a sampling rate of 3 frames per second. One assumption made for the data analysis based on the geometry of the trilayer and based on visual observation was that the temperature mostly propagated down the length of the trilayer. A constant temperature profile was assumed for the width of the trilayer. A mean temperature value was calculated by averaging the values of a 10 pixel wide strip down the length of the trilayer. Surface plots were used

[3]Princeton Applied Research, www.princetonappliedresearch.com

to represent the spatial and temporal progression of the temperature of the trilayer [4].

3.4 Results

During the trilayer heating experiments, one frequent observation made was that the voltage signals applied across the thickness of the trilayer caused the the copper electrical contacts to short through the ion permeable membrane. This caused the temperature at the base of the trilayer clamped by the electrical contacts to sharply jump to a value outside the range of the infrared camera which was set to a maximum of 440 K, while the rest of the trilayer stayed at room temperature. In an attempt to avoid degrading the trilayers during actuation, a different configuration for the electrical contacts was used (Figure 3-4(b)) in which the pair of electrical contacts needed to actuate the trilayer was separated. Electrical contacts were placed at opposite sides and opposite ends of the trilayer to prevent the current from shorting directly between the two copper strips.

3.4.1 Single pulse actuation

Results from the single pulse tests show the temperature profile of trilayer actuated with different voltage steps. Both the single contact and double contact configurations were used to activate the trilayers. The signal sent from the potentiostat was a series of 4 single low frequency pulses of increasing voltage. Each voltage was applied for 5 seconds and turned off for 15 seconds. Figure 3-5 is a collection of the data taken from the single pulse test. Electrochemical data is presented as well as the temporal and spatial distribution of temperature in the trilayer. For display purposes, the time scale on the 3-dimensional plots increases from right to left. The two sets of data correspond to the tests performed in the single-end contact configuration and the double-end contact configuration. The two graphs in Figure 3-6 clarify the

[4] All Matlab code written to analyze and process the data captured by the Thermovision infrared camera can be found in the attached DVD

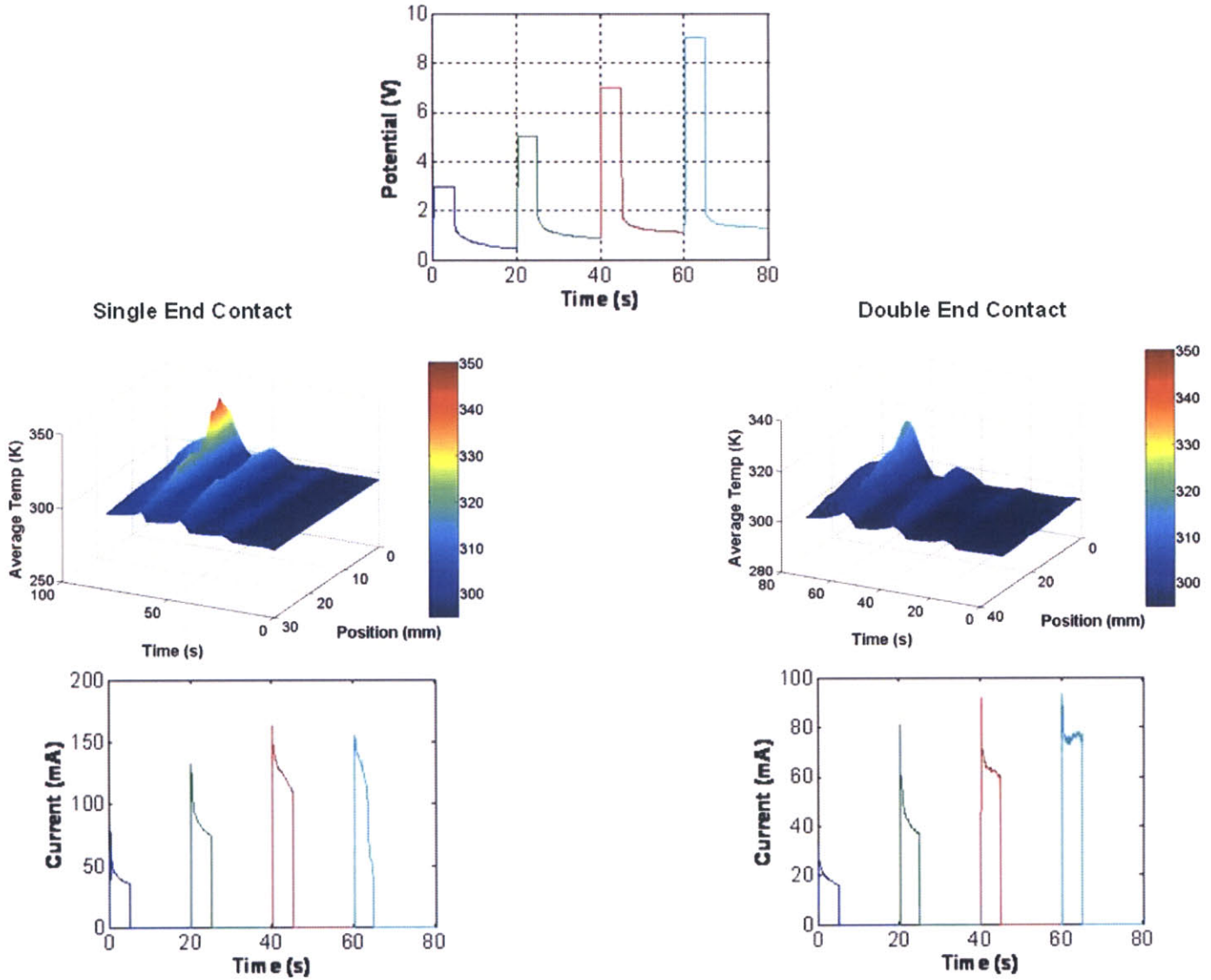

Figure 3-5: Single Pulse Actuation - Top: Voltage profile used to activate trilayer; Middle: Temporal and spatial distribution of temperature of the trilayer activated with both contacts at one end (left) and both contacts at opposite ends (right) For display purposes, the time scale on the 3-dimensional plots increases from right to left.; Bottom: Corresponding current profiles of each trilayer during actuation. Temperature scales are equal for both 3-D plots and range from 295 K to 350 K.

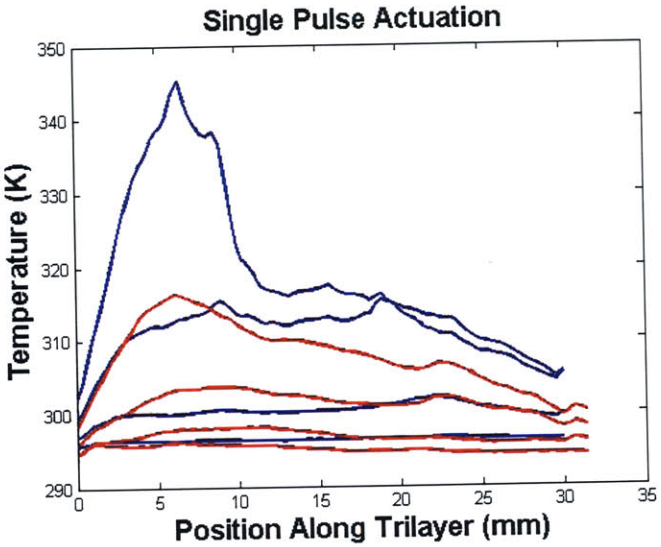

(a) Temperature profiles along the length of the trilayer at the end of each 5 second pulse. Blue lines indicate single ended contact. Red lines indicate double ended contact. Profiles of increasing magnitude correspond to the increasing voltages used

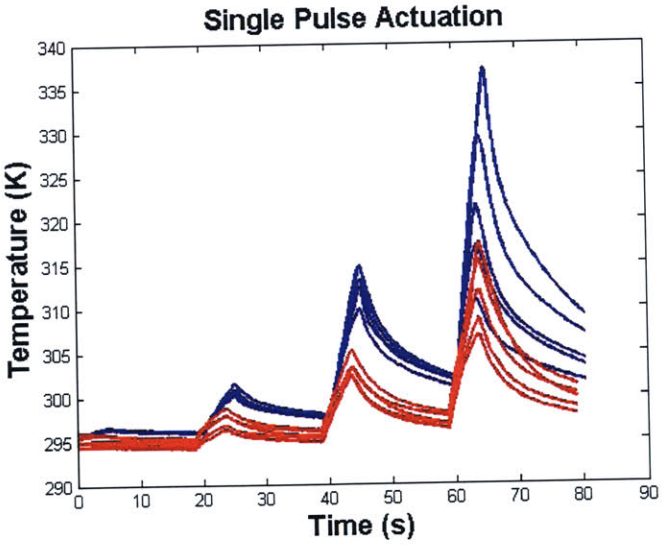

(b) Temperature profiles over time at 5 points along the length of the trilayer (5, 10, 15, 20, and 25 mm from the base of the trilayer). Profiles decrease from 5mm to 25mm. Blue lines indicate single ended contact. Red lines indicate double ended contact.

Figure 3-6: Temperature profiles along the length of the trilayer and over time.

temperature profiles over time and along the length of the trilayer.

One difference that is apparent from the graphs in Figures 3-5 and 3-6(a) is that the trilayer activated with double ended contacts lacks the large jump in temperature in the 9 Volt step that is present in the trilayer that is activated with single ended contacts. Polymer resistance plays a large role in the propagation of voltage down the length of the trilayer. At low voltages, the voltage drop along the polymer is small. This is evident in Figure 3-6(b) with the 3, 5, and 7 Volt pulse tests. The temperature profiles at the 5 points along the trilayer are very closely spaced which suggests that there is not a large voltage drop down the length of the trilayer. In the 9 Volt test however, the temperature profiles are spaced further apart indicating a large voltage drop between each of the points. At the higher voltages the finite conductivity of the film in the trilayer caused the injected charge to build up near the points of contact resulting in a high charge density which overheated the trilayer. In contrast, the two ended contact was able to distribute the injected charge and avoid localized overheating. This is evident in the current profiles of each trilayer. The current drawn by the trilayer with double ended contacts is half the current drawn by the trilayer with single ended contacts.

3.4.2 Low frequency actuation

Results from the low frequency actuation tests show the temperature profile of a trilayer actuated with a 0.25 Hz signal. Both single and double contact configurations were used to activate the trilayers. The signal from the potentiostat was a series of four 0.25 Hz cycles of ± 3, 5, 7, and 9 Volts. Figure 3-7 is a collection of the data taken from the low frequency tests. Electrochemical data is presented as well as the temporal and spatial distribution of temperature in the trilayer. For display purposes, the time scale on the 3-dimensional plots increases from right to left. The two sets of data correspond to the tests performed in the single-end contact configuration and the double-end contact configuration. The two graphs in Figure 3-8 clarify the temperature profiles over time and along the length of the trilayer.

The 3-D plots in Figure 3-7 show an obvious effect that electrical contact place-

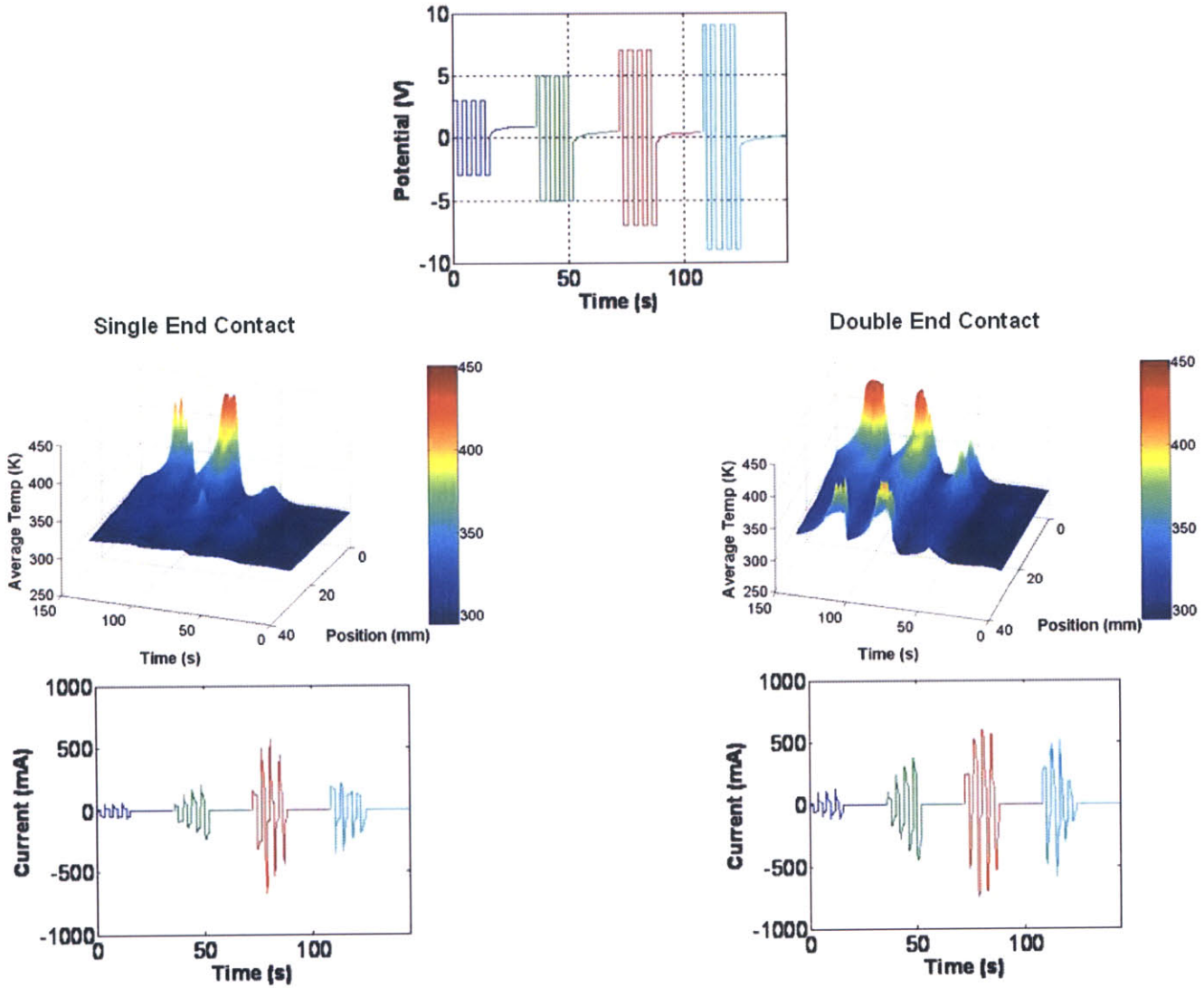

Figure 3-7: Low Frequency Actuation - Top: Voltage profile used to activate trilayer; Middle: Temporal and spatial distribution of temperature of the trilayer activated with both contacts at one end (left) and both contacts at opposite ends (right) For display purposes, the time scale on the 3-dimensional plots increases from right to left.; Bottom: Corresponding current profiles of each trilayer during actuation. Temperature scales are equal for both 3-D plots and range from 295 K to 450 K.

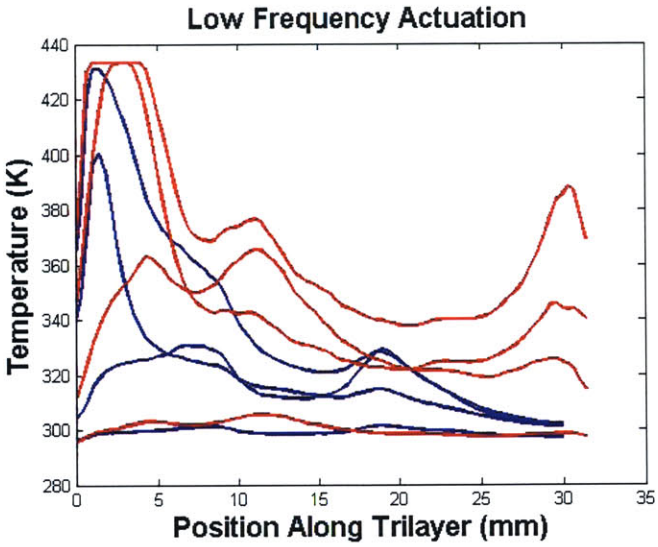

(a) Temperature profiles along the length of the trilayer at the end of 4 cycles at 0.25 Hz. Blue lines indicate single ended contact. Red lines indicate double ended contact.

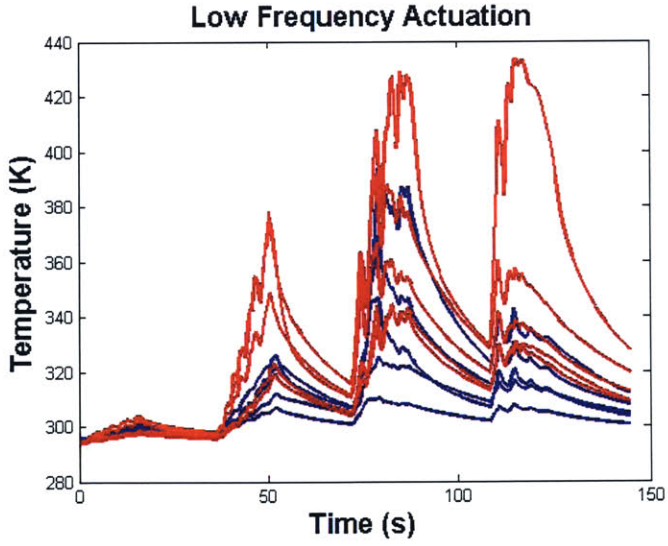

(b) Temperature profiles over time at 5 points along the length of the trilayer (5, 10, 15, 20, and 25 mm from the base of the trilayer). Profiles of increasing magnitude correspond to the increasing voltages used. Blue lines indicate single ended contact. Red lines indicate double ended contact.

Figure 3-8: Temperature profiles along the length of the trilayer and over time.

ment has on the heating behavior of a trilayer. The voltage drop along the polypyrrole was significant in both cases. Spikes in the temperature profile occurred near the electrical contacts. Driving the trilayer with a 0.25 Hz low frequency signal heated the trilayer proportionally to the applied voltage. The ±7 Volt and ±9 Volt signal exceeded the limits of the trilayer, degrading the portion of the trilayer near the contacts. The double contact configuration was able to raise the temperature of the central portion of the trilayer to a higher temperature than the trilayer in the single contact configuration. Unlike the single pulse actuation, the trilayer with double ended contacts heated up more than the one driven with the single ended contacts. Degradation of the single-end contacted trilayer from the earlier single pulse tests may have affected its performance in the low frequency tests which explains the lower temperature and the decrease in temperature from the ±7 Volt to the ±9 Volt test.

3.4.3 Varied frequency actuation

In the previous section, a relatively low frequency signal was used to activate the trilayers. At higher voltages, there was a large voltage drop across the polymer which resulted in localized overheating of the trilayers. To look at the effect that signal frequency had, a low voltage cycled at various frequencies was used to actuate the trilayers.

Results from the varied frequency actuation tests show the temperature profile of a trilayer actuated with a ±2 Volt signal cycled at 0.5, 5, 50, and 500 Hz. Figure 3-9 is a collection of the data taken from the low frequency tests. Electrochemical data is presented as well as the temporal and spatial distribution of temperature in the trilayer. For display purposes, the time scale on the 3-dimensional plot increases from right to left. Only the single ended electrical contacts were used in these tests. The two graphs in Figure 3-10 clarify the temperature profiles over time and along the length of the trilayer.

A low 2 Volt signal was used to prevent overdriving the trilayer. However, this actuation scheme failed to heat the trilayer along the length of the trilayer. From Figure 3-10(a), it is evident that heating only occurs within the first 5 mm of the base

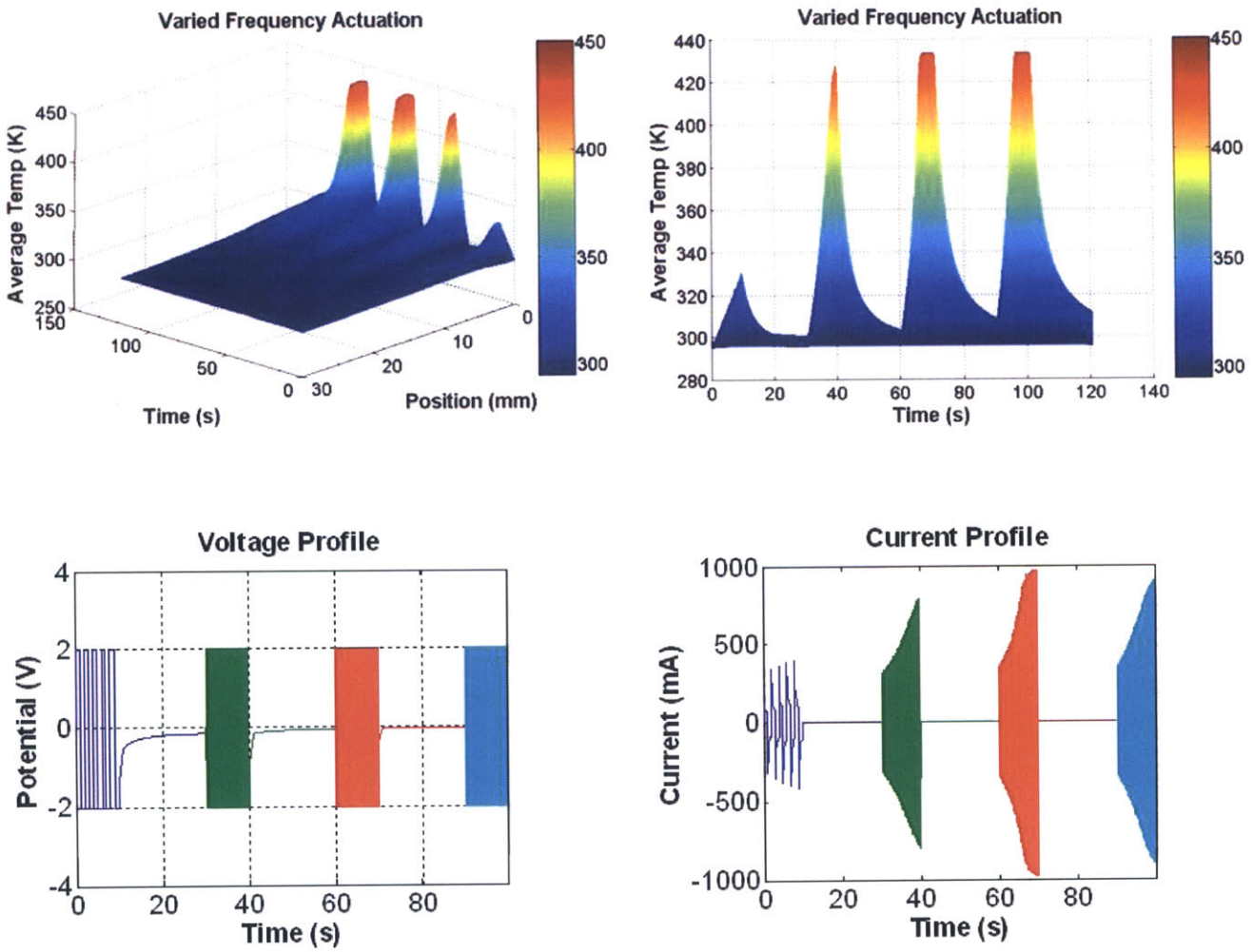

Figure 3-9: Varied Frequency Actuation - Top: Temporal and spatial distribution of temperature of the trilayer, Isometric view (left) and Front view (right). For display purposes, the time scale on the 3-dimensional plots increases from right to left. Temperature scales are equal for both plots and range from 295 K to 440 K; Bottom: Voltage profile used to activate trilayer (left) and corresponding current profile (right).

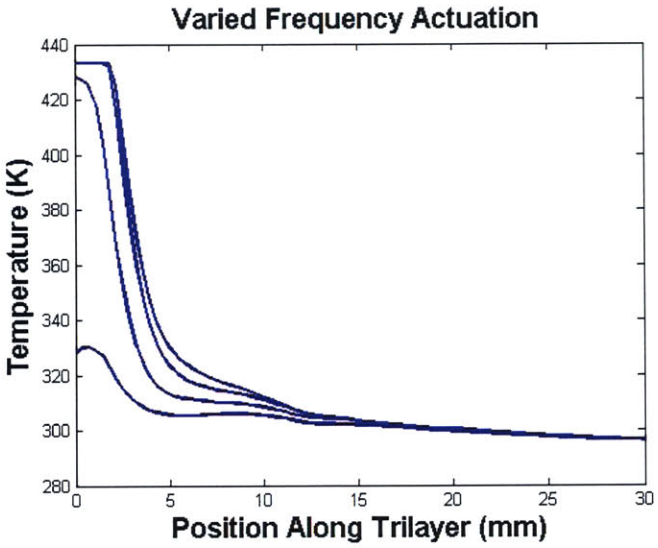

(a) Temperature profiles along the length of the trilayer at the end of 10 seconds of cycling ±2 Volt at 0.5, 5, 50, and 500 Hz. Profiles of increasing magnitude correspond to the increasing frequencies used

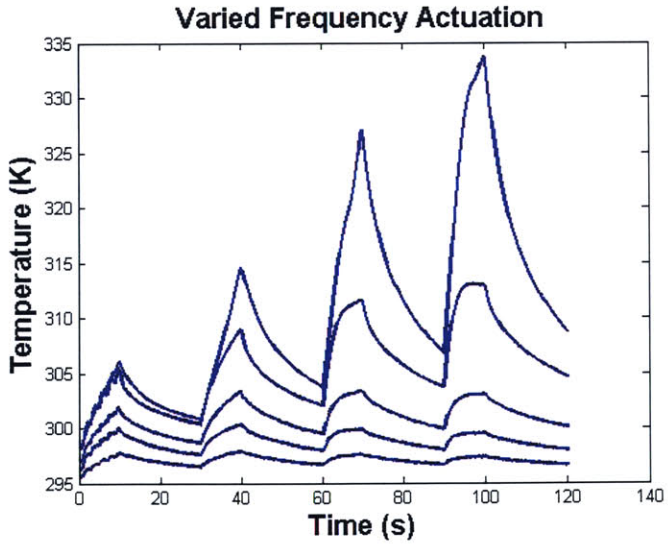

(b) Temperature profiles over time at 5 points along the length of the trilayer (5, 10, 15, 20, and 25 mm from the base of the trilayer. Profiles decrease from 5mm to 25mm.

Figure 3-10: Temperature profiles along the length of the trilayer and over time.

of the trilayer. Figure 3-10(b) shows that increasing the signal frequency increases the rate in change of temperature at the base of the trilayer. However, this temperature spike only occurs at the base and does not propagate down the length of the trilayer. The trilayer seems to short across the ion permeable layer at high frequencies of 5, 50, and 500 Hz.

3.4.4 Discussion

From the results presented in the previous section, some important trends can be extracted. Including a separation between electrical contacts allows one to heat the area of the trilayer between the contacts more evenly to a higher temperature and avoids localized heating just at the base of the trilayer. The magnitude of the voltage applied is proportional to the amount of joule heating that occurs in the trilayer. Because of the proportional relationship between voltage and temperature, there is also a relationship between the frequency of an applied signal and the distance the temperature propagates down the length of the trilayer. For a set distance spacing between electrical contacts, a low frequency signal will result in more even heating because the polymer is able to equilibrate to the applied potential. If the distance between the electrical contacts is shortened, the frequency required for even heating increases. Conversely, if the distance between the electrical contacts is lengthened, the required signal frequency for even heating must be decreased. For specific applications, if the frequency of actuation is known, the spacing between the electrical contacts can be determined achieve the best temperature profile.

Because of the effect that the finite conductivity of the polypyrrole films has on the voltage profile along the length of the strip, there is a relationship between the signal frequency and the maximum allowable voltages that could be applied to the trilayer at those frequencies. At low frequencies, the applied voltage has more time to equilibrate along the entire trilayer which results in more even temperature profiles. At higher frequencies, the voltage applied must be lowered to decrease the voltage drop along the polypyrrole, allowing the charge to be evenly distributed during the shorter time.

One must be reminded that during actuation, the power consumed by the trilayer is not always converted to heat. Some of the power contributes to the mechanical power required for the volumetric change in the polypyrrole. However, in the case of the heating experiments that were discussed in this chapter, motion of the trilayer was restricted, preventing any mechanical work from being done. Also, with the magnitude of the driving signals used in these experiments, the percentage of the power converted to mechanical work would have been minimal since the efficiency with which electrical energy is converted to mechanical energy is on the order of a couple percent for polypyrrole [17]. Heating in the trilayers can be avoided by keeping the applied voltages or currents low. However the following chapters help to explain why the heating behavior may be desirable.

Chapter 4

Temperature Effects

A correlation seemed to exist between temperature and the performance of trilayers. To identify the cause of the improvement in trilayer actuation, it was necessary to isolate the different components of the trilayer to see how the rise in temperature affected each one. The following sections describe the experiments performed to test the mechanical, electrical, and electrochemical properties of the electrolyte gel, the liquid ionic salt, and the polypyrrole film at different temperatures.

4.1 Temperature effects on electrolyte gel

Electrolyte gel samples used in the experiments were mixed according to the recipe listed in Table 2.1. Both mechanical and electrochemical tests were carried out to determine the effect of temperature on the modulus and ionic conductance of the electrolyte gel.

4.1.1 Mechanical properties of gel

Experimental Method

To prepare the samples for mechanical testing, electrolyte gel was placed in an acrylic well with a Teflon base(Figure 4-1(a)) and cured in an oven at 85 °C for 30 minutes. Once cured, a punch was used to cut out a 13 mm round sample (Figure 4-1(b))

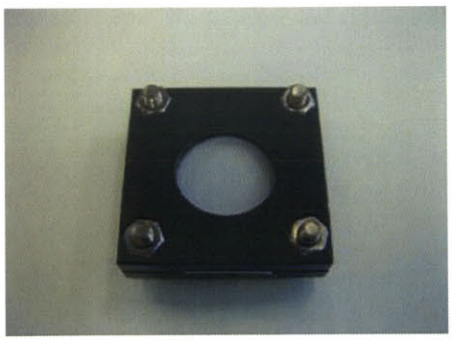

(a) Acrylic cell used to prepare electrolyte gel sample for mechanical testing.

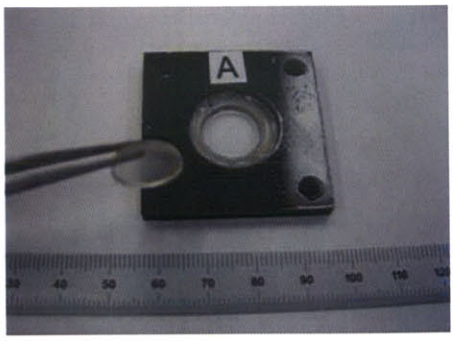

(b) Round sample used for mechanical testing.

Figure 4-1: Sample preparation for mechanical testing.

Compressive tests following ASTM standards [1] depicted in Figure 4-2 were carried out on the cylindrical gel samples to determine the modulus using a PerkinElmer [1] DMA 7e dynamic mechanical analyzer. The analyzer was equipped with the cup and plate measuring system, which had a 20 mm cup mounted at the base and a 18 mm top parallel plate. The electrolyte gel samples were loaded in the cup while the parallel plate probe was lowered onto the surface of the sample.

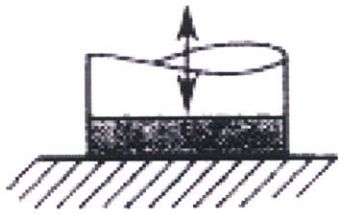

Figure 4-2: Dynamic compression testing method. Source: [1]

The 7 Series Thermal Analysis Software was programmed to apply a static force of 1.54 N with a superimposed dynamic force of 770 mN at a frequency of 1 Hz. Forces were applied over the area of the 13 mm diameter sample, or 113 mm^2. During the dynamic compression testing, the sample was held at 25 ^oC for 5 minutes before starting the heating process. The sample was heated from 25 ^oC to 100 ^oC at

[1] PerkinElmer, www.perkin-elmer.com

3 °C/min, held at 100 °C for 1 minute, and cooled from 100 °C to 25 °C at 3 °C/min.

Results

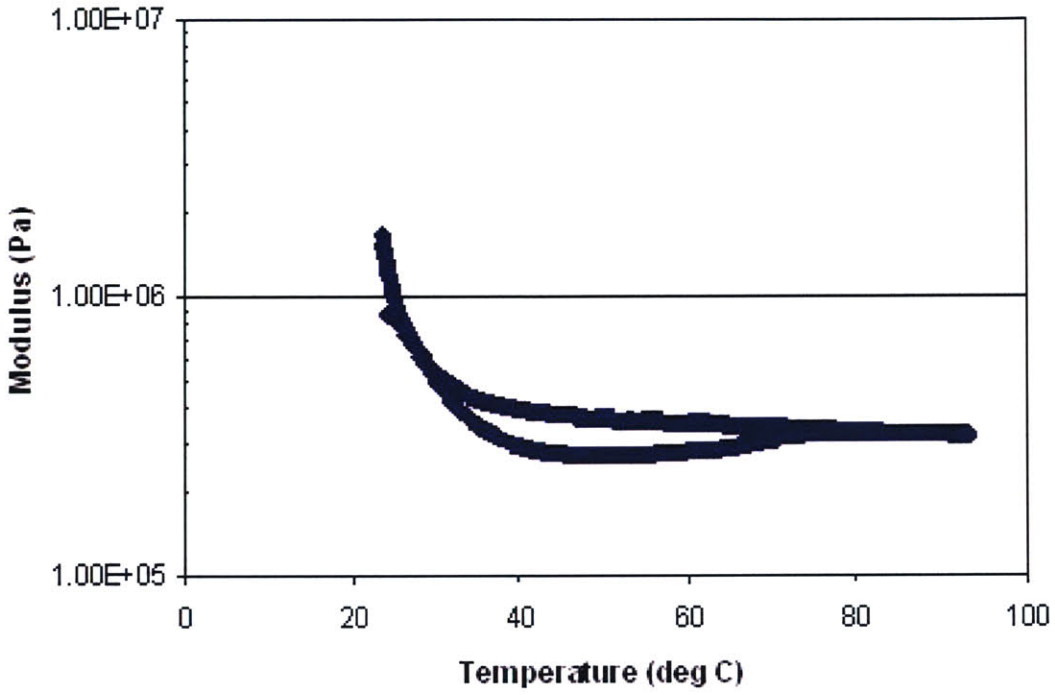

Figure 4-3: Effect of temperature on electrolyte gel modulus.

Several samples of $BMIMBF_4$ electrolyte gel were tested. Figure 4-3 displays the modulus of one sample plotted on log scale. Elastic modulus drops by an order of magnitude, indicating a glassy transition phase around room temperature above which the gel has relatively higher mobility. The modulus reaches a plateau as temperature is further increased. The initial modulus of the electrolyte gel at room temperature is around 2 MPa. This value drops to 0.3 MPa for temperatures above 40 °C.

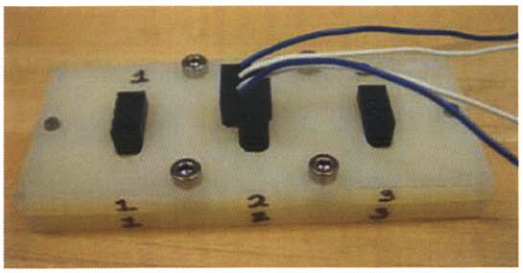

(a) Experimental set-up used to take 4-pt resistance measurements.

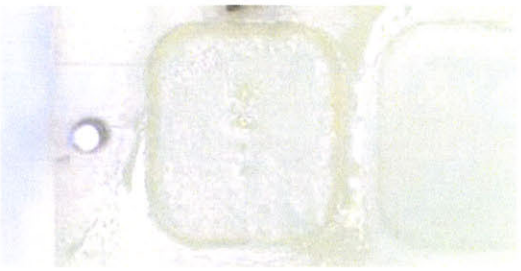

(b) Electrolyte gel sample in nylon test bed.

Figure 4-4: Sample preparation for ionic conductance testing.

4.1.2 Ionic admittance of gel

Experimental Method

To prepare the samples for electrochemical impedance testing, electrolyte gel was cured at 85 °C for 30 minutes in shallow wells machined in a nylon block seen in Figure 4-4(b). Once cured, a four-pronged terminal header block was lowered to slightly penetrate the surface of the thin layer of gel. The two outer pins were used to apply a potential and the two inner pins were used to measure the resulting current (Figure 4-5). The four point approach was taken to eliminate errors due to contact resistance. Liquid salt samples were also prepared for impedance testing by the same procedure minus the curing step.

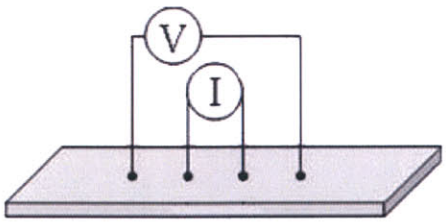

Figure 4-5: Electrolyte gel ionic conductance testing method. Courtesy of Nate Vandesteeg.

Electrochemical impedance spectroscopy was performed on the samples using a

VMP2 Multichannel Potentiostat [2]. Samples were heated to various temperatures in a CSZ MicroClimate Series Environment Simulation Temperature Chamber [3].

The potentiostat was programed to perform electrochemical impedance spectroscopy on the samples by applying a 10 mV peak to peak oscillation about 0 volts at frequencies from 100 kHz to 100 mHz at 10 points per decade and taking 3 measurements per frequency. The impedances at each temperature were relatively steady over the frequency range swept except for the low frequencies which require sustained ionic migration. Excluding the high impedances at the low frequencies, the values were averaged to get an overall impedance at each temperature. The inverse of the impedance was taken to give a value for electrolyte gel admittance.

Results

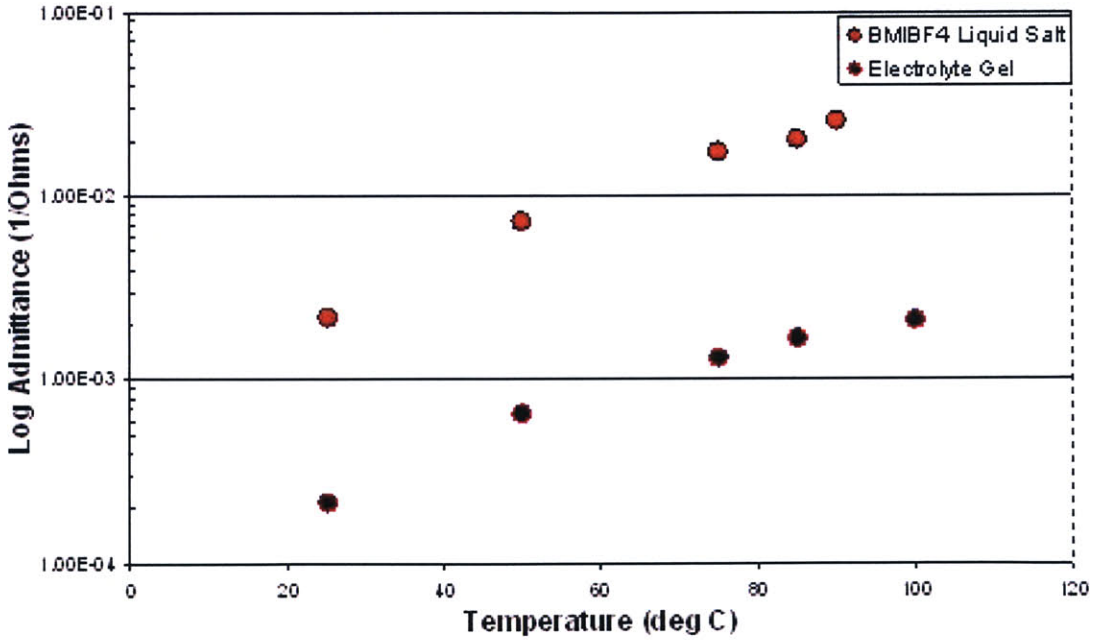

Figure 4-6: Effect of temperature on the ionic admittance of electrolyte gel and liquid salt.

The admittance is plotted against the inverse of the temperature. The electrolyte

[2]Princeton Applied Research, www.princetonappliedresearch.com
[3]Cincinnati Sub-Zero, www.cszindustrial.com

gel has a lower admittance than the liquid salt by itself, but both show the same temperature dependance. The order of magnitude difference between the conductances can be attributed to the additional polymer matrix of the electrolyte gel partially immobilizing the movement of ions.

The temperature dependent behavior of the admittance of the electrolyte gel and liquid electrolyte behaves as expected according to Gray. The ionic conductivity of liquid and solid electrolytes versus temperature can be approximated by the Arrhenius equation [10], which describes the temperature dependence of a system:

$$\alpha = A \exp\left(-\frac{E}{T}\right), \tag{4.1}$$

where A is a exponential factor specific to the particular system property being measured, which in this case is the admittance, and E is an activation energy.

4.2 Temperature effects on polymer actuation

All experiments done exploring temperature effects on polypyrrole were carried out by Mike Del Zio and are detailed in his thesis [8]. The following are graphs that show the passive and active properties of polypyrrole at different temperatures.

4.2.1 Passive properties of polypyrrole

Figure 4-7 is taken from Mike DelZio's studies on the effect of temperature on the passive properties of polypyrrole. During the first ramp in temperature, the modulus of the polypyrrole increases with temperature. As the temperature is brought back down to room temperature, the modulus continues to increase. The modulus versus temperature curve reaches a state of equilibrium with subsequent temperature cycles. After the initial increase verses temperature, the modulus of polypyrrole seems to be inversely proportional to temperature. The modulus of polypyrrole dropped by more than a third of its original value as the temperature was increased from 25 ^{o}C and 125 ^{o}C.

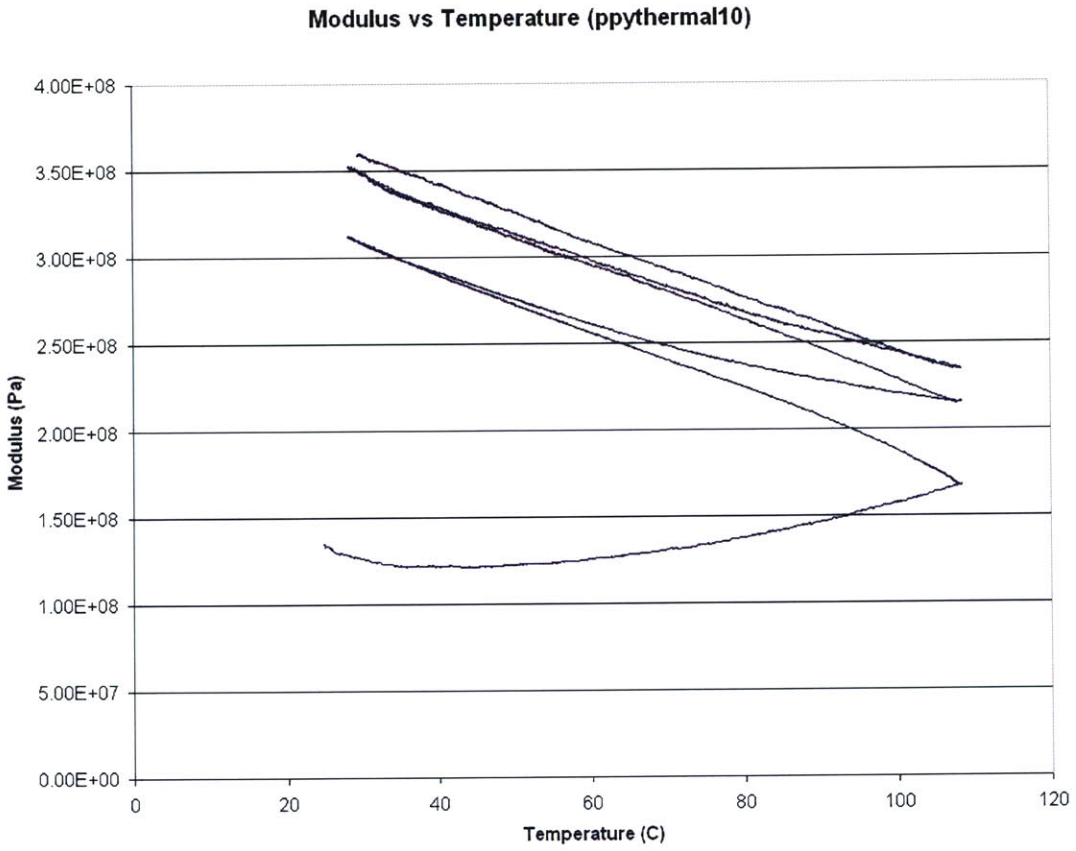

Figure 4-7: Modulus of a strip of polypyrrole as it is being cycled between 25 ^{o}C and 125 ^{o}C. Source: [8].

4.2.2 Active properties of polypyrrole

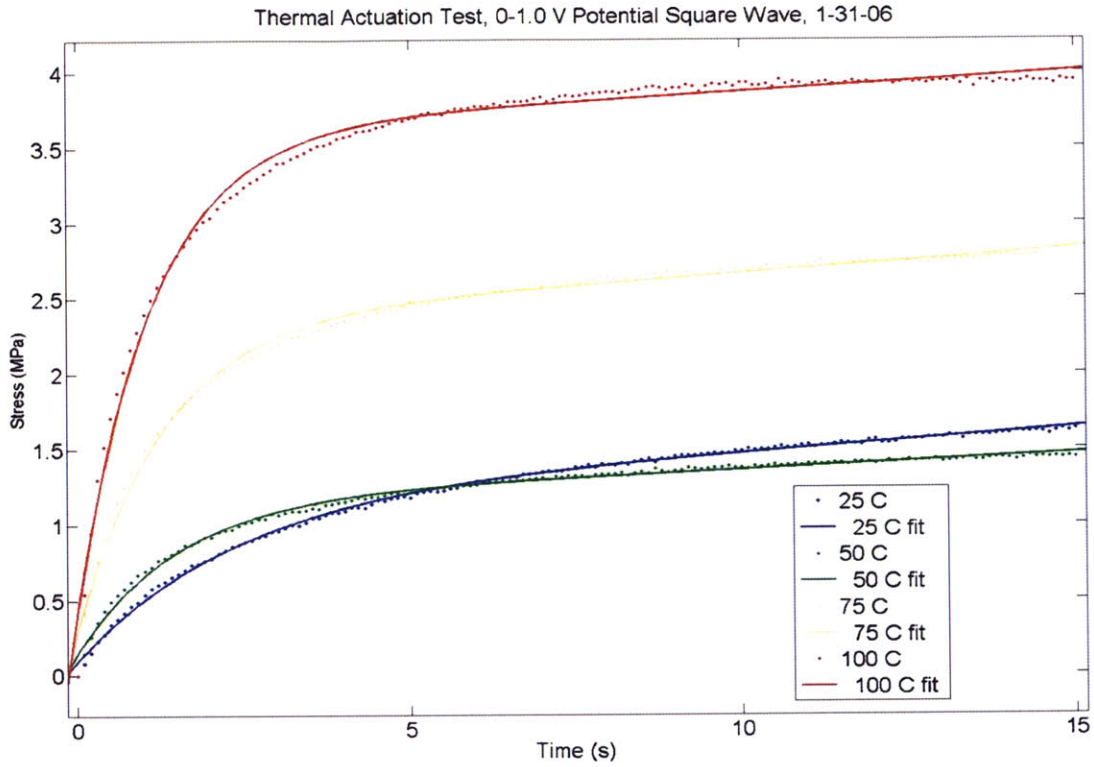

Figure 4-8: Thermal actuation tests done on polypyrrole at 25 °C, 50 °C, 75 °C, and 100 °C. Source: [8].

Figure 4-8 is also taken from DelZio's thermal studies on polypyrrole. In these tests, a strip of polypyrrole was submerged in an electrolyte bath and actuated at 25 °C, 50 °C, 75 °C, and 100 °C. According to the graph, the stress rate produced by the strip of polypyrrole stayed constant between 25 °C and 50 °C. However, between 50 °C and 100 °C, the stress rate increases and maximum stress produced increase with temperature. These curves were fit to an exponential with two time constants corresponding to the diffusion time constant, τ_D, and the resistive time constant, τ_{RC}.

4.3 Discussion

All of the results presented in this chapter help to explain how the thermal behavior affects the different components of the trilayers mechanically, electrically, and elec-

trochemically. In addition, they help to support the observations made about the increased speeds of actuation and the the large displacements that occur. To understand how the temperature dependent properties affect the performance of the trilayers, one must look at the governing equations and time constants describing the motion of trilayers, which were presented in Sections 1.2 and 1.3.

In Section 1.3, the equations describing the internal stresses experienced by the polypyrrole and the electrolyte gel were presented. The stress gradient across the thickness of the trilayer resulted in an internal bending moment. The curvature produced by the internal bending moment induced by the strain in the polypyrrole layers was ultimately dependent on the stiffness of the trilayer structure. The flexural rigidity of the trilayer is given by the equation

$$EI = E_p I_p + E_g I_g \,, \tag{4.2}$$

where I is the area moment of inertia for the strips of polypyrrole and the layer of electrolyte gel.

According to the results, the modulus of the electrolyte gel drops by an order of magnitude as it is heated and reaches a plateau of 0.35 MPa at temperatures above 40 °C. There was an initial increase in the modulus of the polypyrrole during the first temperature scan. However, this change in modulus occurs occurs during the fabrication process described in Chapter 2 when the trilayer was baked in the oven at 85 °C. During actuation, the modulus of the polypyrrole is inversely proportional to temperature. In one temperature scan from 25 °C to 125 °C, the modulus of the polypyrrole dropped to two-thirds its original value. In Madden's diffusive elastic model, elastic modulus has no effect on the strain to charge ratio. However, having a low elastic modulus does result in larger passive displacement in response to an applied load, whereas a high elastic modulus will reject such disturbances [23]. Both of these decreases in the modulus of the polypyrrole and the electrolyte gel in response to temperature contribute to reducing the flexural rigidity of the trilayer, which affects the resulting curvature and helps to explain the increasingly large displacements seen

during actuation as the trilayer heats up.

Looking at the three time constants that are important in assessing polymer actuator performance (Equations 1.1, 1.2, and 1.3), one can see that the diffusion coefficient, D, and electrolyte conductivity, α_e both have an effect on the speed of actuation in the polypyrrole. The results presented in this chapter show that both of these variables change with temperature. The ionic conductivity is essentially a measure of the mobility of the ions within the methacrylate matrix. Its behavior can be approximated by the Arrhenius equation. During actuation, polypyrrole undergoes strains via ions diffusing into th bulk of the polymer. The results from Figure 4-8 show that strain rates of the polypyrrole and thus ion diffusion rates increase with increasing temperature. Diffusivity often obeys the Arrhenius Law in many cases [25]. The Arrhenius law applied to diffusivity is given by the equation:

$$D(T) = D_0 e^{-\frac{E_a}{RT}}, \tag{4.3}$$

where $D(T)$ is the diffusion coefficient as a function of temperature, D_0 is the theoretical maximum diffusion coefficient at infinite temperature, E_a is the activation energy for diffusion, R is the universal gas constant, and T is the temperature.

The diffusion coefficient is inversely proportional to τ_D and τ_{DDL} which describe the diffusion of ion into the polymer and through the double layer. Therefore, increasing the temperature during actuation increases the diffusion coefficient, which in turn increases the speed of actuation.

Electrolyte conductivity, α_e, is inversely proportional to τ_{RC} which describes the charging time of the double layer at the electrolyte/polypyrrole interface. Therfore, increasing the temperature during actuation increases the ionic conductivity, which increases the double layer charging time.

Chapter 5

Force Production

The compact packaging that allows trilayers to be actuated in air, makes it easier to integrate these actuators into larger systems. Possible applications such as active surface control will be discussed in Chapter 6. However, in order to assess whether or not the trilayer actuator is a feasible option for a certain application, it is important to know the force output of the actuator. In the model that Madden used to predict force output of trilayers [23], certain parameters such as the strain to charge ratio, α, polypyrrole and gel layer thicknesses, h_p and h_g and polymer modulus, E_p, were assumed to remain constant. From the discussion in Chapter 4, it is apparent that these parameters change as a function of temperature. Therefore, the parameters are never constant since the process of actuating the trilayers results in self heating of all the components. Previous studies have tried to increase trilayer force output by stacking the actuators in parallel [23]. The biggest problem in the stacked configuration was the mechanical interference between trilayers. To accomodate the different motions of each trilayer, flexible hinge points were used at the tips of the trilayer to allow unhindered rotation at the hinges. This chapter will show that force output can be increased via heating, whether it is induced by joule heating or by changing the environment in which the trilayer is actuated.

In addition, many studies that look at force production of bending actuators focus mainly on force production at the tip of the actuator. In the experimental setup described in Section 5.1, tip force is not measured. Instead, force over an

area is measured. This may seem counterintuitive at first because the trilayer is a bending actuator. However, possible applications of these trilayers include underwater propulsion in AUV's. Therefore, the important parameter is not the force produced right at the tip, but instead the average thrust produced by the entire surface of the trilayer.

5.1 Experimental Setup

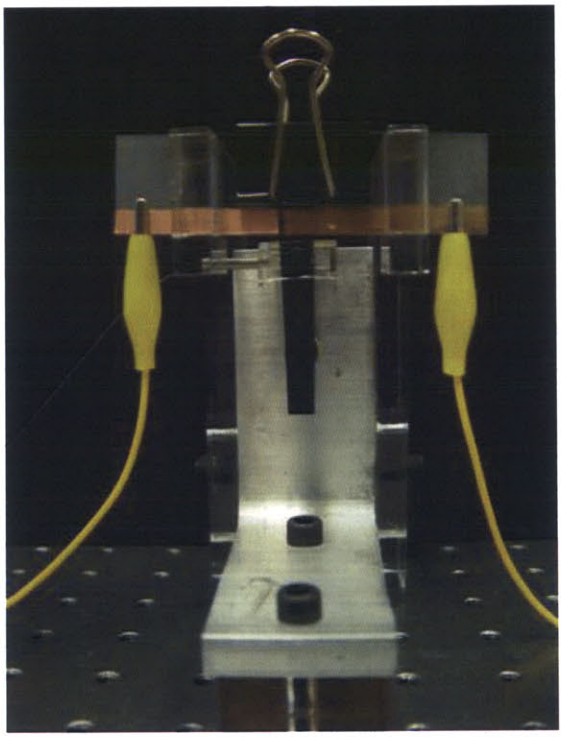

Figure 5-1: Force setup with trilayer clamped in load cell. Yellow clips send in electrical signal.

The experimental setup used to measure force output of trilayers is shown in schematically and physically in Figure 5-1. The trilayer being tested was sandwiched between two glass slides (Figure 5-2) with copper tape providing the electrical contact where the signal was being sent in. The binder clip was used to ensure a good electrical contact between the copper tape and the trilayer. Care was taken not to let the copper tape on the glass slides touch each other to avoid shorting the circuit. The glass slide

assembly was inserted in the two slots in the top arms of the force setup to hold the trilayer in a vertical configuration.

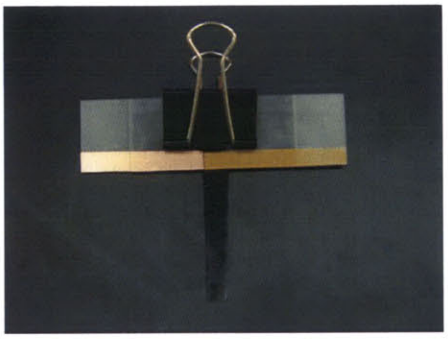

Figure 5-2: Trilayer clamped between two glass slides to make electrical contact.

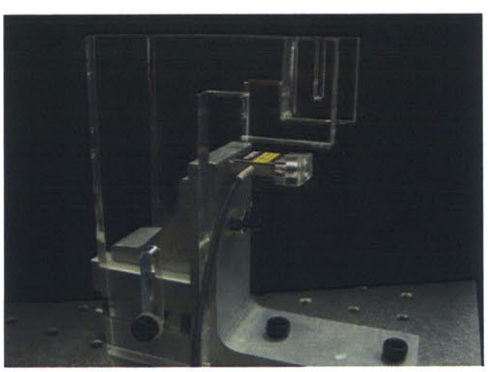

(a) Force setup with load cell.

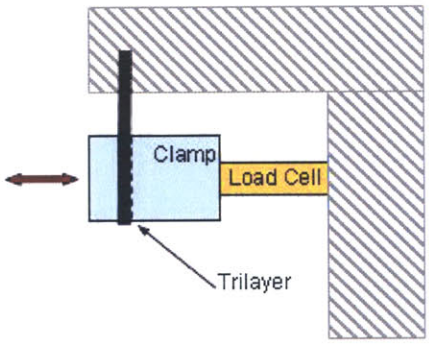

(b) Schematic of force setup.

Figure 5-3: Physical and schematic setup for force measurement.

The section of the trilayer right below the glass slides is secured by a clamping block which was attached horizontally to a fixed load cell (Figure 5-3). Trilayers were cut to size 10 mm wide and 18 mm long. A 6 mm section of the trilayer was clamped in the glass slides to make electrical contact. The remaining section of the trilayer was held in the clamping block. The trilayer was trimmed so that the end of the trilayer coincided with the end of the clamping block to eliminate any overhang. This would ensure that all the charge injected into the trilayer would go into actuating the section held by the clamping block. The clamping force used was just tight enough eliminate

any slop but not tight enough to mechanically impede the conducting polymer layers from contracting and expanding. The area of the clamp on which the trilayers were exerting force was a 10 mm by 10 mm area.

In some experiments, trilayers were artificially heated with an external source such as a heat lamp.

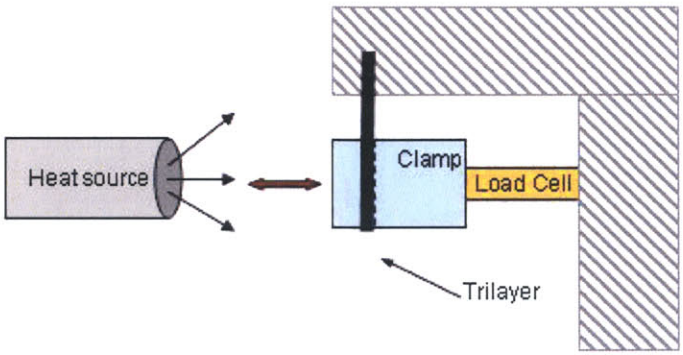

Figure 5-4: Schematic setup for force measurement with heat source.

The voltage and current signals were sent and recorded by the VMP2 Multichannel Potentiostat [1]. The signal from the load cell was sent through a signal conditioning amplifier and readings were recorded using a National Instruments DAQPad-6052E [2] [3]. For some experiments a K-type thermocouple from Omega [4] was clamped in with the trilayer to observe the approximate heating behavior of the trilayer during actuation. These readings only capture the appoximate thermal behavior because they only show the temperature of the trilayer at one location. For complete temperature profiles of the trilayer during actuation, refer to Chapter 3. Thermocouple readings were recorded using an Agilent 34970A Data Aquisition Unit [5].

[1] Princeton Applied Research, www.princetonappliedresearch.com

[2] National Instruments, www.ni.com

[3] All Visual Basic and Matlab code written to collect and process data can be found on the attached DVD

[4] Omega, www.omega.com

[5] Agilent, www.home.agilent.com

5.2 Results

Trilayers were actuated at room temperature using many different voltage and current profiles to see force output under different actuation schemes. Data of interest include current profiles, impedance profiles , the force output, and the temperature reading taken by the thermocouple on the surface of the trilayer during actuation.

5.2.1 Effect of trilayer impedance on performance

Several experiments were performed at room temperature to try to relate the force output of the trilayer to its electrochemical and temperature profile. However, a common problem encountered during the experiments was that the behavior of the trilayer at room temperature was unpredicatable due to the variances in the quality of trilayers tested. Some trilayers actuated better than others. The following are results from 3 different tests performed on 3 different trilayers. The trilayers tested in the first two experiments were low impedance, fast actuating trilayers, drawing maximum currents of a couple hundred milliamps. The trilayer tested in the third experiment had a higher impedance, drawing a maximum of only 10 milliamps.

Low impedance trilayer actuated with a ± 9 Volt Potential Square Wave at 2 Hz

Figure 5-5 shows the temperature, force, current, and impedance of a trilayer actuated at room temperature with a 9 Volt square wave at a frequency of 2 Hz. According to Figure 5-5, the trilayer seems to have a warm up period. The impedance across the polypyrrole films at room temperature through the electrolyte gel starts at 400 Ohms. The double layer charging time, τ_{RC}, is large because ion mobility is low. As the potential is cycled back and forth, a small current flows through the polypyrrole gradually heating it via joule heating. As the polypyrrole heats slowly, its mechanical, and electrochemical properties change as well as those of the electrolyte gel. According to the results discussed in Chapter 4, as the temperature rises, the modulus of the gel decreases exponentially and the ionic conductivity electrolyte exponentially increases.

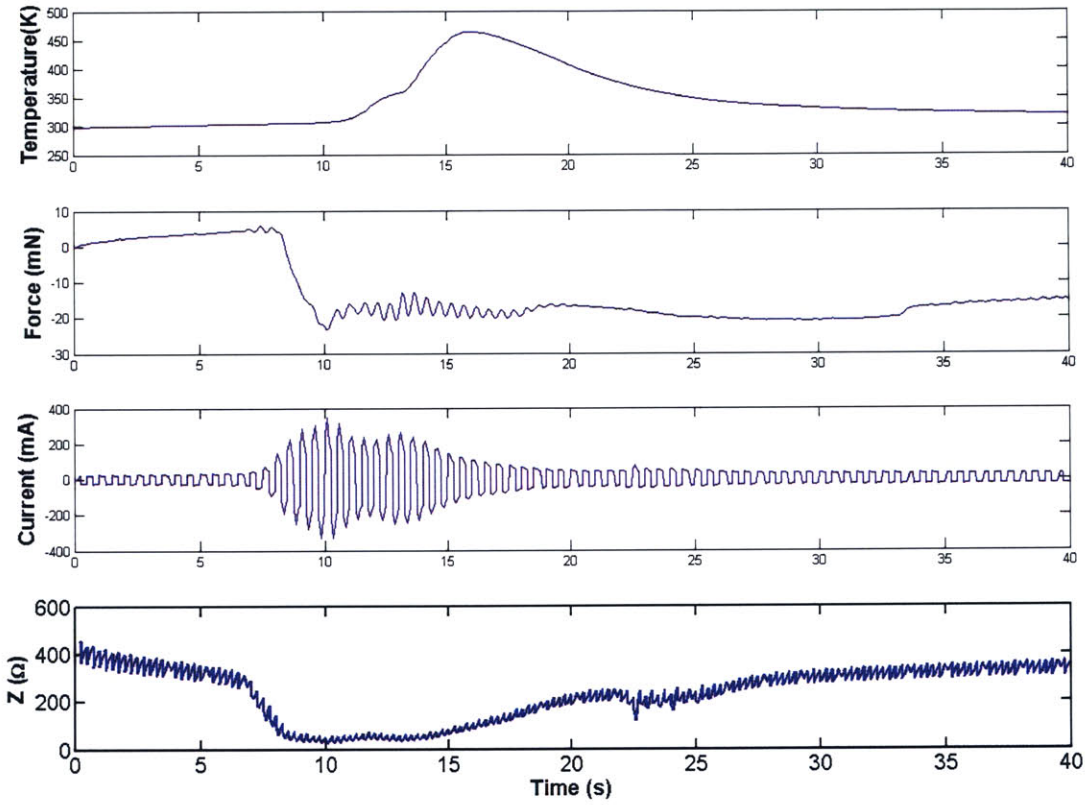

Figure 5-5: Current, temperature, and force output of a trilayer actuated with a 2 Hz $\pm$ 9 Volt square wave at room temperature.

The speed of response of the polypyrrole increases with temperature. According to Equation 1.9, the force profile should follow the charge profile. During the first 7 seconds the magnitude of the response of the polypyrrole is small because the frequency of the charge profile lies outside of the bandwidth of the polypyrrole's actuation capabilities. Most of the charge injected into the polymer contributes to the charging of the double layer capacitance. There is a gradual change in the force due to slight differences in the τ_{RC}, τ_{DL}, and τ_{DDL} of each layer of polypyrrole.

Between 7 seconds and 10 seconds, there is a sharp jump in the current profile. Increased ion mobility allows ions to brake through the double layer and diffuse into the bulk of the polymer. Visually, it is evident that the diffusion of ions into the bulk of the polymer is not uniform over the entire trilayer. This may be attributed to small differences in the thickness or the surface morphology of the polypyrrole where ions may be more prone to diffuse into. It might also be attributed to areas in the electrolyte gel that have a higher concentration of electrolyte. Figure 2.2 in Section 2-5 shows that the electrolyte gel sometimes has areas of phase separation where the concentration of the liquid salt would be much higher.

Once the ions have broken through the double layer and diffused into the bulk of the polypyrrole, the response speed of the polypyrrole increases. Between 10 seconds and 18 seconds, the frequency of the force response of the trilayer follows the frequency of the voltage profile being applied.

At this point, the impedance of the trilayer drops, and the temperature of the trilayer sharply increases due to joule heating and shorting of the two layers of polypyrrole in some areas of the trilayer. After 15 seconds, the impedence of the trilayer rises again because sections of the polypyrrole have been degraded and the magnitude of the response of the trilayer decreases.

Temperature on the surface of the trilayer reaches a max of 460 K. Current reaches a max of 350 mA. Maximum force output reaches -20 mN for a 10 mm by 10 mm square area of contact.

Low impedance trilayer actuated with ± 9 Volt Potential Square Wave at 0.25 Hz

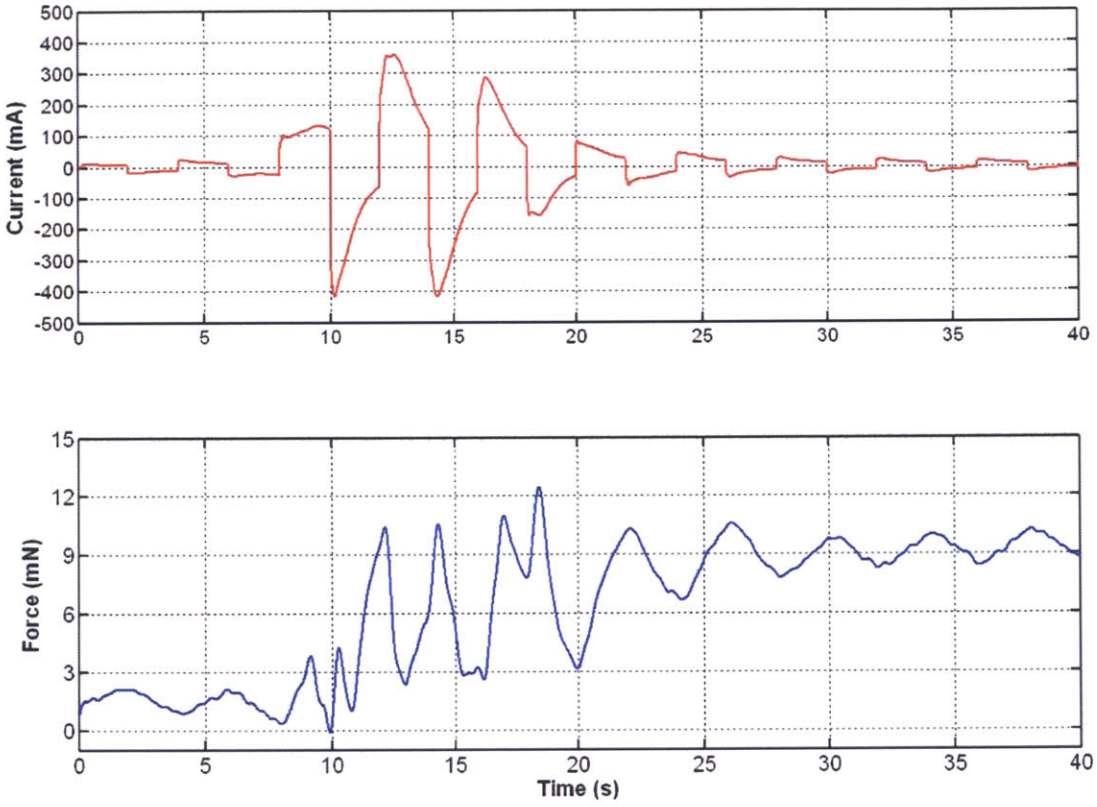

Figure 5-6: Force and current profiles of a low impedance trilayer actuated with a ± 9 Volt Potential Square Wave at 0.25 Hz.

Figure 5-6 shows the current profile and force output of a trilayer actuated at room temperature with a ± 9 Volt square wave at a lower frequency of 0.25 Hz. As seen in the force output graph, the trilayer goes through the same phases. There is a warm up period during the first 7 seconds. Ion mobility spikes and polymer strain rate increases to improve the force output during the next 10 seconds. After some areas of the polypyrrole have been degraded, the current draw and force output decreases. The difference between the performance of this trilayer and the one driven at a higher frequency described in the previous section is that the force output is able to follow the charge density during its warm up state. This is because the frequency at which the trilayer is being actuated is comparable to the rate at which ions can

diffuse into the polymer. In other words, the frequency of the applied potential lies within the bandwidth of the polymer's actuation capabilities.

Maximum current is 350 mA. Force output reaches a maximum of 12 mN.

High impedance trilayer actuated with ± 9 Volt potential square wave at 0.25 Hz

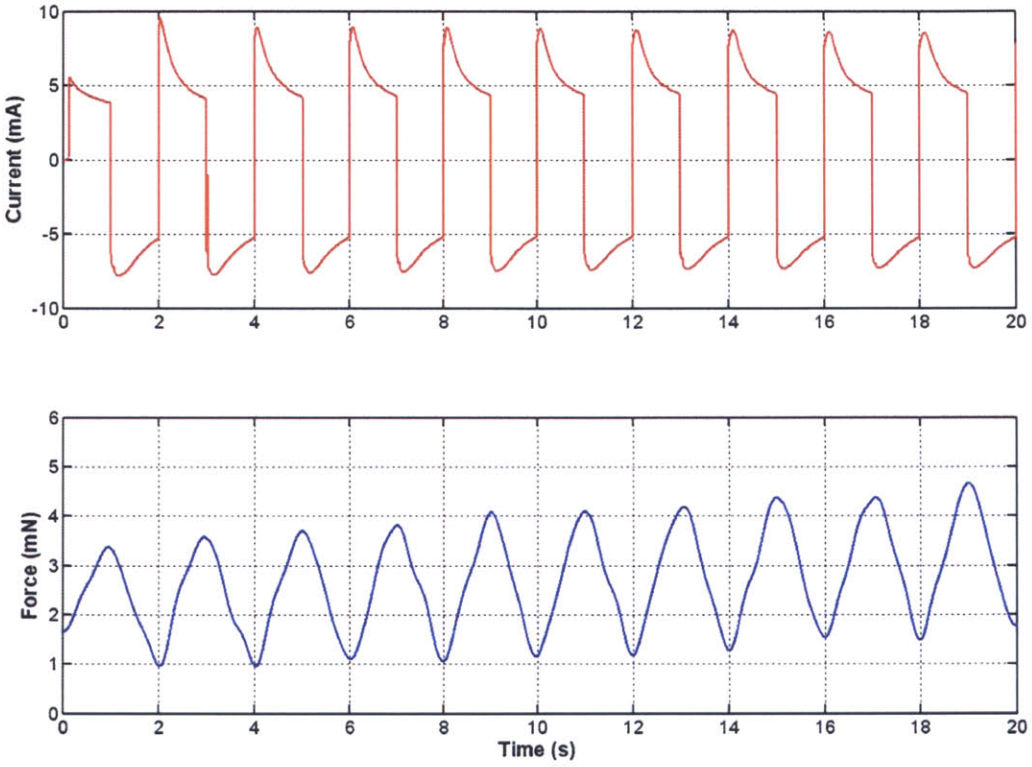

Figure 5-7: Force and current profiles of a high impedance trilayer actuated with a ± 9 Volt square wave at 0.25 Hz

Figure 5-7 shows the current profile and force output of a trilayer actuated at room temperature with a ± 9 Volt square wave at a lower frequency of 0.25 Hz. This trilayer does not exhibit the same warm up, current spike, and degradation phases as the trilayers described previously. The high impedance of the trilayer and the low frequency of the voltage profile do not succeed in heating the trilayer. Therefore the large forces seen in the previously discussed trilayers are not observed in this trilayer. The peak force reached is 4.5 mN. The number of repeatable cycles is increased.

5.2.2 Actuating trilayer with duty cycles versus voltage steps

It was difficult to achieve repeatable results from the actuation schemes describes in Section 5.2.1. Applied potentials were high because fast strain rates were desired. However, it was difficult to predict the degradation voltage due to the variances in trilayer impedance. To prevent degradation of the films during actuation, pulse width modulation was used to control the amount of power that was delivered to the trilayer. This reduced the amount of resistive loss incurred in the polypyrrole. Actuating a trilayer with ±9 Volt pulses at 30% duty cycle, meaning it was 9 Volts 30% of the time and off the other 70%, was equivalent to actuating the trilayer with a ±2.7 square wave. The difference is that the electrochemical impedence across the trilayer was much lower when using the pulse width modulation actuation scheme, because the larger voltage amplitude charged the double layer more quickly and resulted in faster actuation. The short pulses reduced the amount of unnecessary heating of the trilayer that occurs after the ions diffuse through the double layer. Figure 5-8 shows the difference between the impedances of trilayers actuated with square wave signals of different voltage magnitudes (Figure 5-8(a)) and trilayers actuated at different equivalent voltages achieved by varying duty cycles (Figure 5-8(b)). For these tests, actuation frequency was 0.5 Hz with signal polarity switching once every second. This was the rate at which signal polarity was switched. For the duty cycle tests, the pulsing frequency was 25 Hz. Therefore, 9 Volt pulses of vary durations would occur every 0.04 seconds for one second and then switch to -9 Volt pulses. In the trilayer actuated by square waves of various voltage magnitudes, impedance falls as voltage magnitudes rise. At ±0.9 Volts, the impedance starts off at a very large value between 1.5 and 2.5 kOhms. Hardly any actuation occurs at these impedance levels. The voltage is too low to allow ions to charge and diffuse through the double layer. As the voltage magnitude increases, impedances fall and approach an impedance of 500 Ohms. Actuation occurs at the larger voltages and lower impedances. In the trilayer actuated by varying duty cycles, impedance stays constant throughout the actuation process between 250-350 Ohms. Impedance was low even when the equivalent voltage

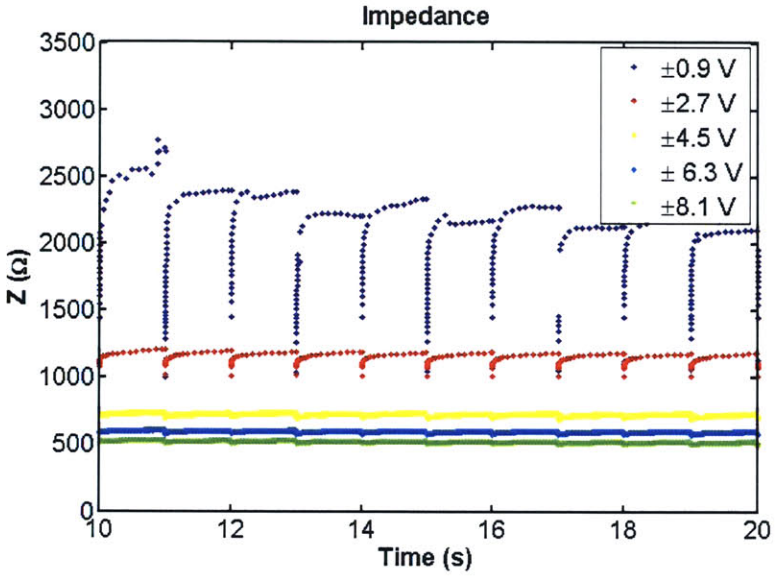

(a) Trilayer actuated with varying voltage steps.

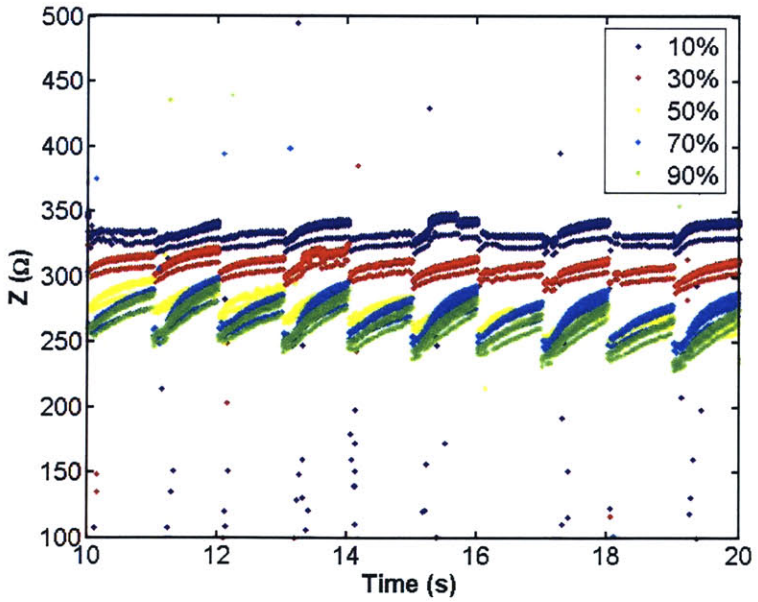

(b) Trilayer actuated at varying duty cycles of ±9 volt pulses.

Figure 5-8: Impedance of trilayers under two different actuation schemes.

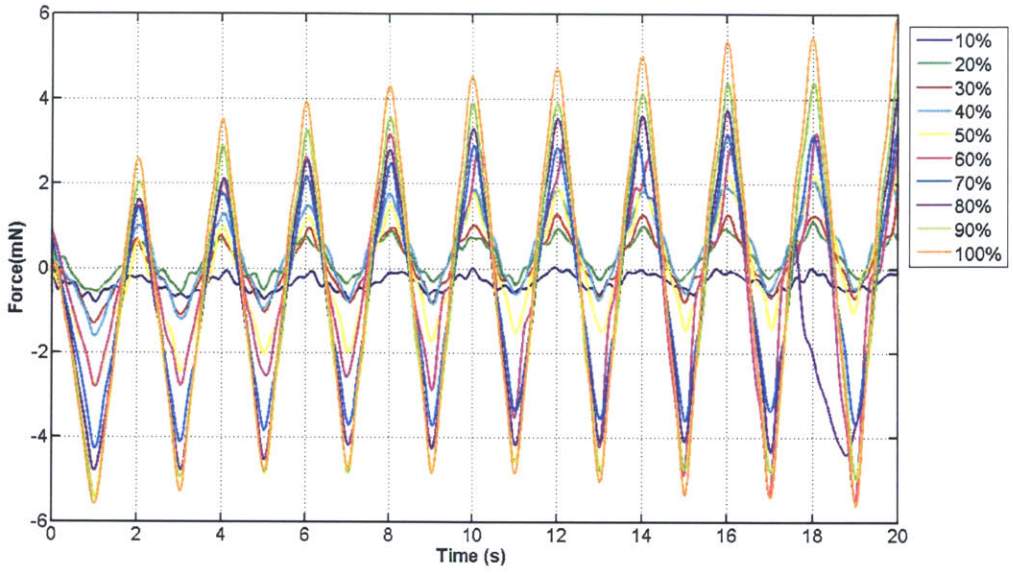

Figure 5-9: Force output of a trilayer actuated with 9 Volt pulses at different duty cycles.

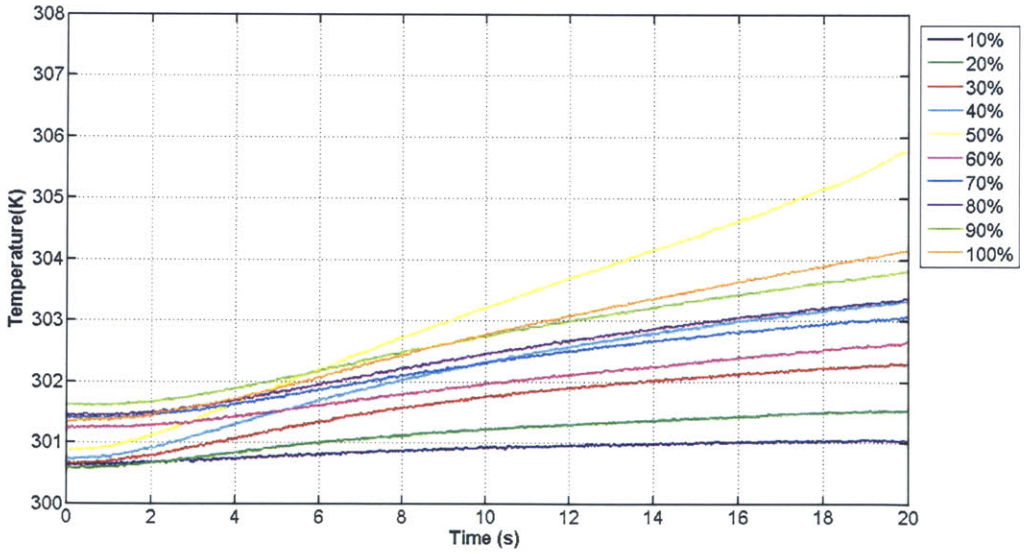

Figure 5-10: Heating behavior of a trilayer actuated with 9 Volt pulses at different duty cycles.

applied was low.

Force profiles for the trilayers actuated with varying voltage magnitudes were, in general, very noisy and did not follow any particular pattern that corresponded with the input signal that was used to drive them. In contrast, the trilayers driven with varying duty cycles followed their input nicely and exhibited a proportional relationship between force and force rate versus increasing duty cycle and power. Unlike the results shown early in Figures 5-5 and 5-6 where force output was often unpredictable and erratic once the ions had broken though the double layer, Figure 5-9 shows a force profile that is very consistent and repeatable. The range of force being produced starts cycling between -6 mN and 2.5 mN and increases to a range between -6 mN and 6 mN. The maximum force rate is 12 mNs^{-1}. The gradual increase in force rate over time, seems to coincide with the gradual increase in temperature that occurs in the trilayer (Figure 5-10).

5.2.3 Artificially heated trilayers

It has been shown that trilayers actuated at room temperature start off at a state of high impedance due to factors such as high gel modulus and low ion mobility. It is difficult to predict the number of cycles they need to reach their low impedance state because it depends on the quality of the polymer and how easy it is for the ions to break through the double layer and diffuse into the polymer. Actuating trilayers with pulses of relatively large voltages at varying duty cycles is an effective way to reduce the impedance of a trilayer while at the same time avoiding degradation of the trilayer. However, there is still room for improvement in terms of the force output and the force rate. This was seen in the experiments in Section 5.2.1 where trilayer were able to achieve maximum forces of 20 mN. Currently, the signals that are used to drive the trilayers are open loop. There is no feedback relaying information on the impedance of the trilayer. Therefore, trilayers are either overdriven and overheated to the point of degradation, or they are not heated enough. There is a very strong correlation between the temperature of a trilayer and its performance. Actuation at higher temperatures lead to faster strain rates. In an effort to see higher performance

but avoid degradation, trilayers are artificially heated to induce the changes in the electrolyte gel and conducting polymer that would normally occur during the resistive heating.

Artificially heated trilayers actuated with duty cycles

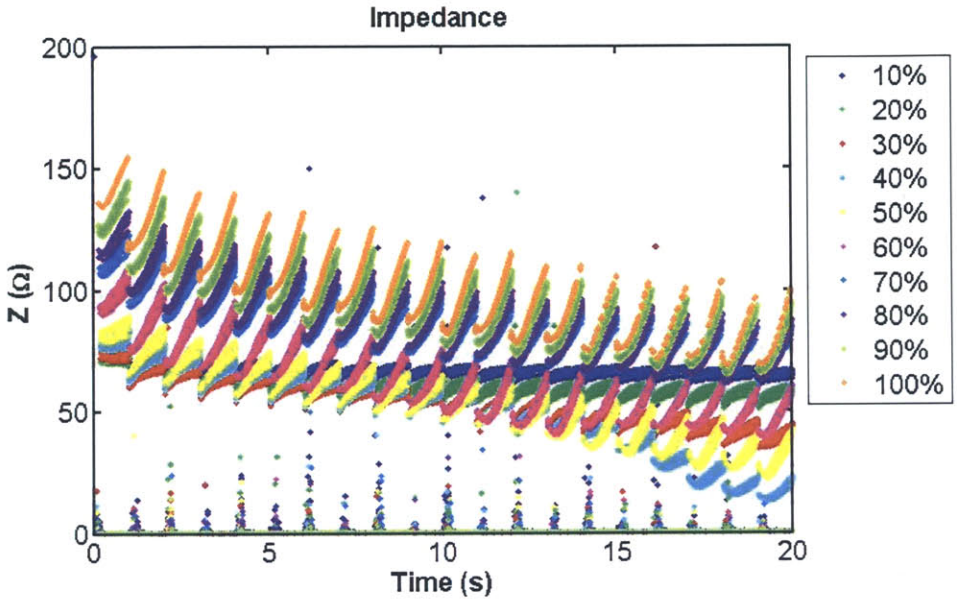

Figure 5-11: Impedance profile for a trilayer that has been artificially heated to 325 K and actuated with ±9 Volt pulses with varying duty cycles.

In this set of experiments, a heat source is placed near the trilayer to artificially heat it to a temperature of 325 K. At this temperature, the modulus of the electrolyte gel is on the lower plateau of its modulus versus temperature curve at 0.3 MPa, and the admittance is increased. Figure 5-11 shows the impedance and Figure 5-12 shows the force output and the rate of force production of a trilayer actuated with 9 Volt pulses pulsing at 250 Hz with varying duty cycles and switching polarity at a frequency of 1 Hz. The impedance lies below the value of 150 Ohms throughout the entire test. For low duty cycles, the impedance of the trilayer stays steady around 70 Ohms. For the duty cycles above 20%, additional joule heating seems to be occuring. The impedance of the trilayer actuated at these duty cycles decreases with time. The impedance reaches its minumum at 40% duty cycle, dropping to 15 Ohms. This

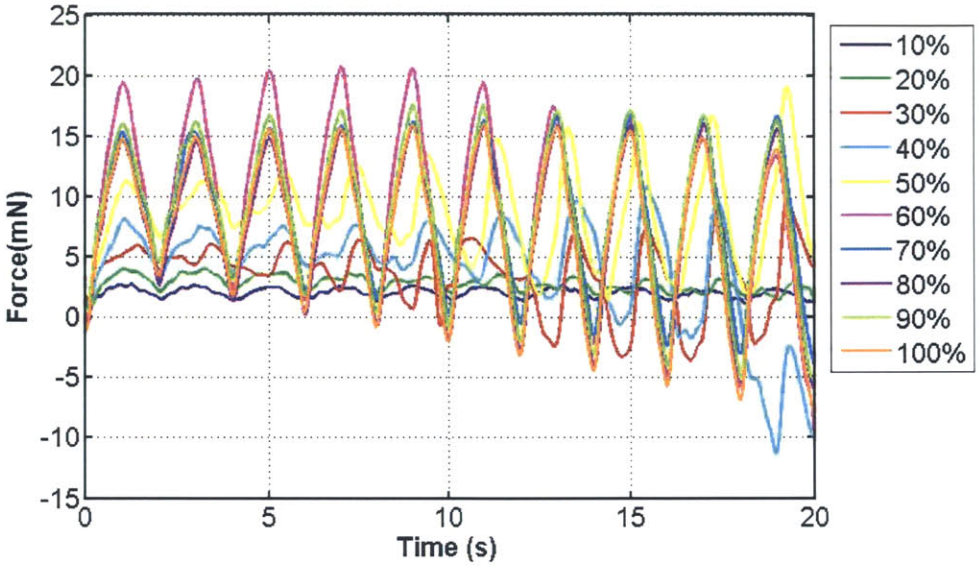

(a) Force output.

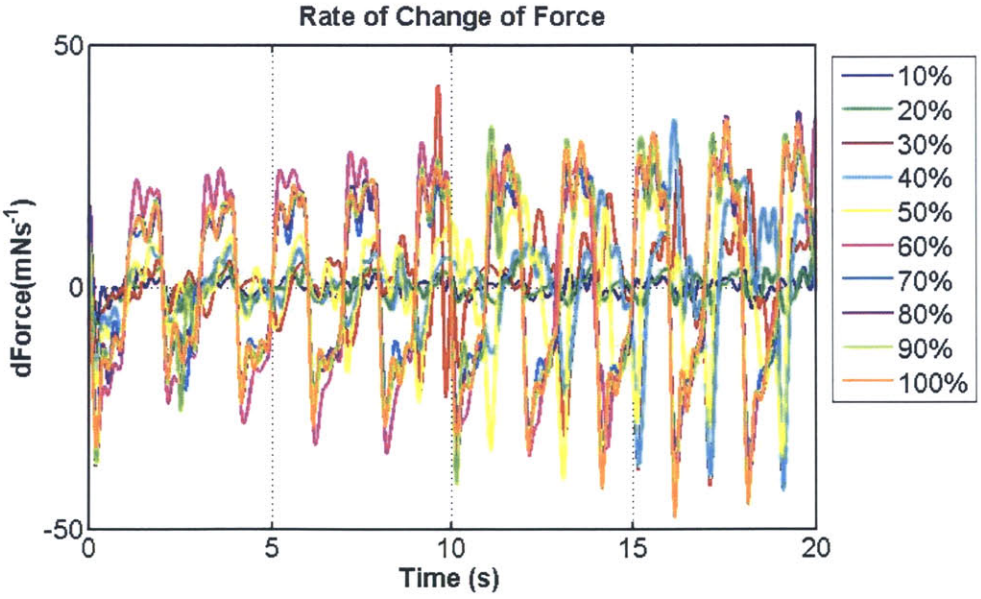

(b) Rate of change of force.

Figure 5-12: Force, and force rate profiles for a trilayer that has been artificially heated to 325 K and actuated with ±9 Volt pulses with varying duty cycles.

also coincides with the large increase in force production and force rate seen at 40% duty cycle. After the 40% duty cycle test, the performance of the trilayer stabilizes. The duty cycle actuation scheme prevents overdriving the polypyrrole. At lower duty cycles, the force output and rate of change of force is relatively low. The magnitude of the force output increases with duty cycle, or equivalent applied voltage. Force output reaches a max of 20 mN at 60% duty cycle and returns to steady maximum of 15 mN after subsequent increases in duty cycle. The $\frac{dF}{dt}$ experiences the largest jump between 50% and 60% duty cycle and seems to saturate around 25 mN/s. The cycles at each duty cycle produce steady, uniform force and $\frac{dF}{dt}$ profiles.

Artificially heated trilayers actuated with a low frequency signal

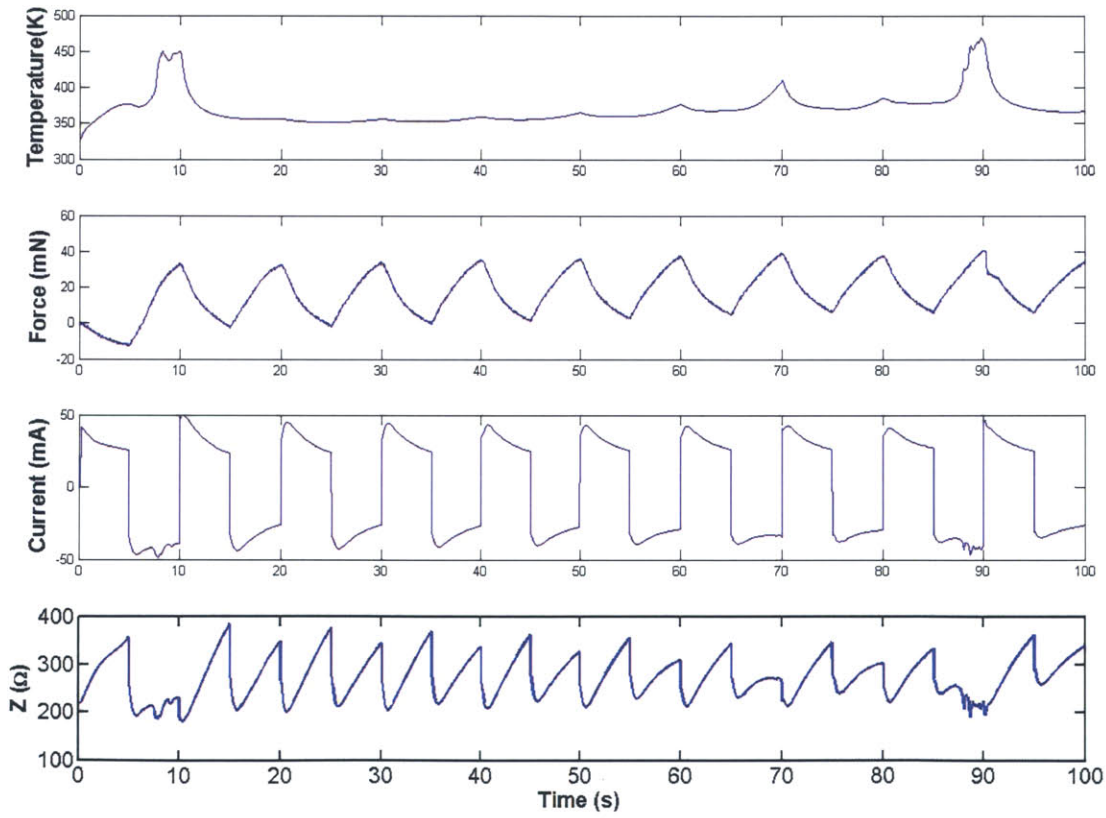

Figure 5-13: Temperature, force, and current profiles of a trilayer actuated with a ±9 Volt potential square wave at 0.1 Hz.

In Chapter 3 it was determined that trilayers could be actuated with higher poten-

tials at lower frequencies without degradation. The longer times allowed the voltage to equilibrate along the length of the trilayer and achieve even temperature profiles. This experiment focused on low frequency signals. A ±9 Volt potential square wave at 0.1 Hz was used to actuate a trilayer. A heat source was used to affect the properties of the electrolyte gel and polymer film. Figure 5-13 shows the improved performance of the trilayer. Other than two spikes in the temperature profile that do not affect the force outputof the trilayer, the temperature rises from its original temperature at 325 K and stays constant at 350 K. The force output is very repeatable and larger in magnitude, reaching a maximum of 40 mN over a 10 mm by 10 mm square area. Impedance during the entire actuation cycle oscillatied between 200 to 400 Ohms.

5.3 Discussion

The results presented in this section illustrate the force capabilities of trilayers. The greatest factor that affects the performance of the trilayers is the overall impedance. The impedance of a trilayer should always be tested before use in any application to ensure its viability as a good actuator. A typical impedance for a fast actuating trilayer should be around 300 Ohms at room temperature. According to Madden, only the charge stored in the capacitance of the polymer contributes to any volumetric changes [19]. The strain is proportional to the voltage across the polymer at equilibrium. Therefore, to maximize strain, it is desirable to maximize the voltage across the impedance of the ions diffusing in and out of the polymer by reducing the series resistance of the electrolyte or reducing its effect [19]. Increasing the applied voltage leads to a faster charging and discharging of the polymer. However, with the series resistance of the electrolyte, there is a risk of overshooting the degradation voltage of the polymer. Minimizing the series resistance is key to preventing overshoot [23]. Based on the results from Chapter 4, temperature has a large effect on the series resistance of the electrolyte gel. Increasing temperature leads to greater ion mobility which lowers the impedance of the electrolyte.

High potential actuation works to improve actuator performance in two ways.

First, it increases the voltage across the double layer capacitance and the bulk capacitance of the polymer which is proportional to the strain. Second, large currents through the resistance of the electrolyte and the polymer dissipate heat. This heat acts to reduce the impedance of the electrolyte which increases the fraction of the applied voltage seen across the bulk capacitance of the polymer resulting in even more strain. This compounding effect produces faster strain rates and rates of force production with every actuation cycle.

The evolution of the series resistance with repeated high voltage actuation cycles is evident in the experiments performed on trilayers at room temperature. The series resistance of the electrolyte in the low impedance trilayer decreased with every actuation cycle resulting in faster rates of force production. In the case where the high impedance trilayer was actuated at room temperature, the series resistance was too high to dissipate any heat. Without the added temperature effect, the rate of force production stayed constant over time.

Driving trilayers at larger voltages lowers the overall impedance. However, there is always the risk of overdriving the trilayers and degrading them. One method of actuating trilayers is to pulse higher voltages across the trilayer with a low duty cycle. This is an alternative to the resistance compensation method developed by Madden [17]. The duty simulates an equivalent lower voltage, but the time constants for double layer charging and ion diffusion are still kept short because of the high voltage that is applied.

The methods of actuating trilayers in this section are all open loop methods. There is no form of feedback to prevent overheating of the trilayers. Trilayers are either overheated, or heated very slowly. Feedback methods to control the temperature were not explored. However Madden's resistance compensation method would be a feasible way to control the amount of heating that occurs in the trilayer. Trilayers were artificially heated to explore the theorectical force capabilities of trilayers if a feedback control loop did exist to control temperature. Results show that a 10 mm by 10 mm section of a trilayer can exert up to 40 mN of force. Maximum rates of force generation are in the range of 25 mN per second for the same size section

of trilayer. These values suggest that trilayers could be a viable actuator to use in many applications including underwater propulusion and maneuvering. Steps taken towards this goal are discussed in Chapter 6

Chapter 6

Potential Applications in Autonomous Underwater Vehicle Technology and Future Work

An area of research which could benefit from conducting polymer trilayer-like actuator technologies is in the discipline-integrated research of biorobotic autonomous undersea vehicles (AUV) in the context of underwater maneuvering and propulsion. In current AUV technologies discussed in [3], mature methods of swimming locomotion based on principles of steady state hydrodynamics have already been developed and are readily implemented. Nature, on the other hand, has taken billions of year to perfect efficient methods of underwater locomotion based on principles of unsteady state hydrodynamics. However, these methods are not often pursued because current actuators are not capable of the high level of control required. One of the goals of research in conducting polymer actuators such as trilayers is eventually to be able to move away from traditional actuators in AUV applications and move towards an actively controlled, dynamic, artificial pectoral fin because of its exceptional capabilities in propulsion and maneuvering. Traditional actuators used in AUVs are rigid and noisy, whereas conducting polymer actuators have the advantages of being lightweight, flexible, and silent.

Increased understanding of the hydrodynamics of fish fin motions has revealed the

huge potential of having flexible active control surfaces instead of discrete actuators. Studies have shown that fish are able to actively control the conformation of the fin by using multiple muscle and tendon attachment points at base of bilaminar fin rays to expand or curve the fin into oncoming flow [14]. Ongoing research focuses on trying to understand the underlying mechanisms of fish fin motions that allow fish to produce thrust The three most prominent modes of thrust producing fin motions include sweep, curl, and cupping. [14], [7]. This chapter focuses on the steps that have been taken to integrate conducting polymers into a fin design to achieve controlled motions, in hopes of moving towards a more biologically-inspired fin design for underwater maneuvering and propulsion. This is an ongoing area of research.

6.1 Active Surface Control

Because improved actuation occurs at higher temperatures, and a large resistive drop along the length of the trilayer causes localized joule heating, joint-like behavior with estimated polypyrrole strain rates on the order of several percent per second is observed near the electrical contact points. The localized heating decreases the modulus of the gel and increases ion mobility, thus improving polymer strain rates along the heated segment. The ability to locally actuate trilayers is a huge step towards achieving an actively controlled surface. Studies in the placement of electrical contacts, mechanical structural elements, and methods of encapsulation for underwater actuation were done to test the feasibility of incorporating conducting polymers in a biologically-inspired pectoral fish fin. Videos supporting the following sections can be found in the attached DVD.

6.1.1 Electrical Contacts

Taking advantage of the finite conductivity of the polypyrrole films, placement of electrical contacts becomes a method of controlling what areas of the trilayer get actuated.

Figure 6-1 shows the hinge-like actuation that occurs in trilayers. From videos

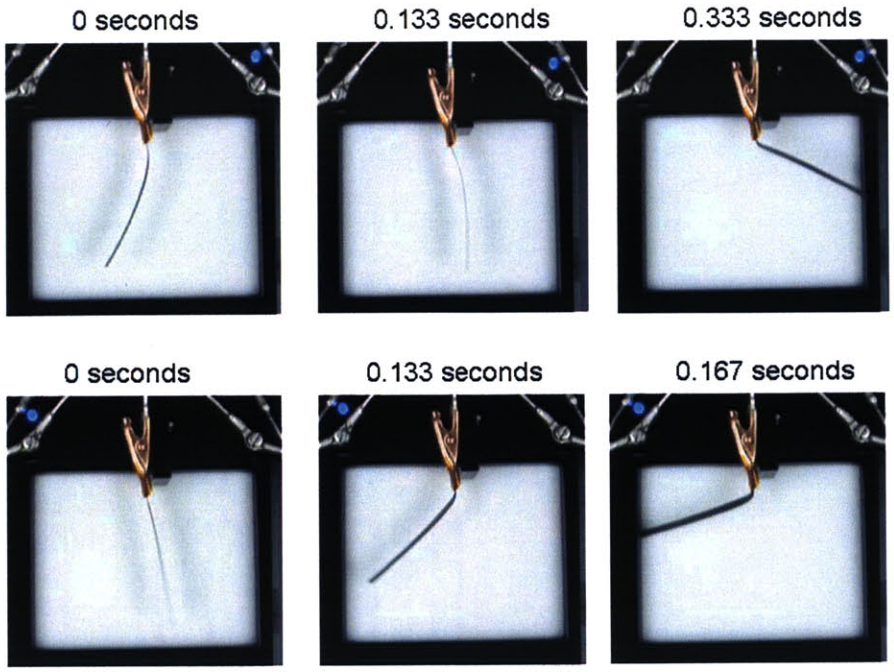

Figure 6-1: Localized actuation near the electrical contacts. Estimated strain rate is on the order of 10% per second.

taken of trilayer actuation, strain rates for the polypyrrole in the hinge-like area have been estimated to be on the order of 10% per second.

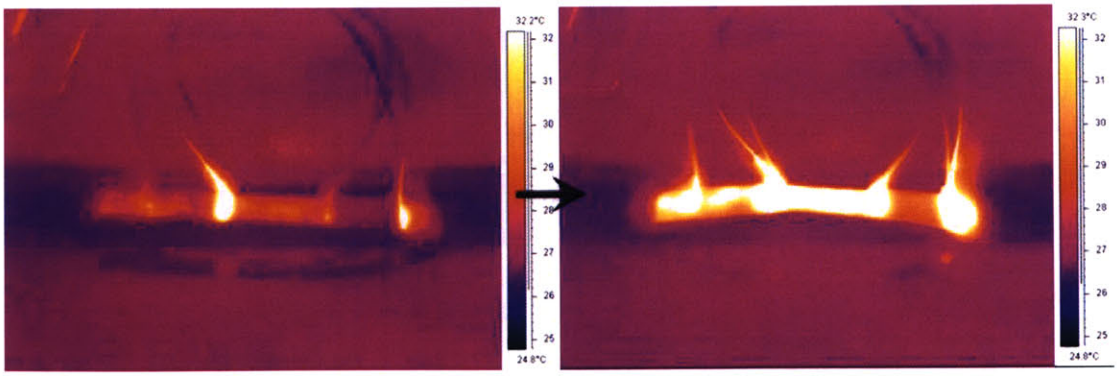

Figure 6-2: Trilayer actuated at 4 different points. Localized heating observed.

In Figure 6-2, pairs of wires (one on each side of the trilayer) were adhered to a trilayer at four distinct points using spray adhesive. All of the wires on each side of the trilayer were joined to form one connection point where the electrical signal could be fed in. Upon actuation under the thermal camera, localized heating was observed

(a) Conductive trace drawn on trilayer.

(b) Trilayer with conductive trace actuated under the thermal camera.

Figure 6-3: Conductive traces used to achieve localized heating.

at the four points of electrical contact. Since the wires adhered to the surface of the trilayer impeded mechanical expansion and contraction of the conducting polymer at those points, the resulting behavior of the trilayer was a hinging motion around the four points of contact.

Conductive patterns were drawn on trilayers to try to locally heat the actuators in a pattern that would result in different actuation configurations other than curling (Figure 6-3(a)). Patterns were drawn with a micro-tip pen used for drawing conductive silver traces on flexible surfaces. Apparent in Figure 6-3(b), the conductive trace drawn on the surface of the trilayer was successful in locally heating the pattern. However, since there were no mechanical constraints applied to the trilayer, The resulting motion, was a curling of the trilayer around the alligator clips clamping the trilayer. Therefore, localized heating must be coupled with mechanical constraint structures in order to achieve active surface control of the trilayer.

The method of hand drawing conductive patterns is not uniform or repeatable. It is also difficult to create complex patterns. Other methods that can be explored to produce better results include metal evaporation deposition techniques. Masks can be used to control gold patterns deposited on the surface of the trilayer.

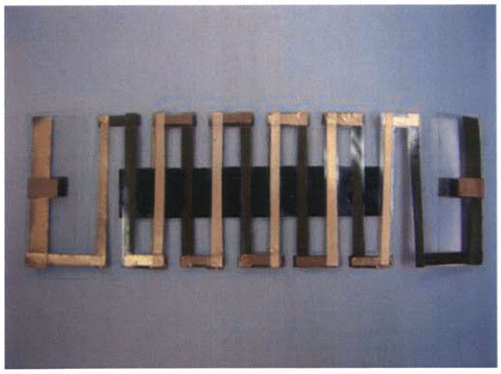

(a) Accordion style flexure.

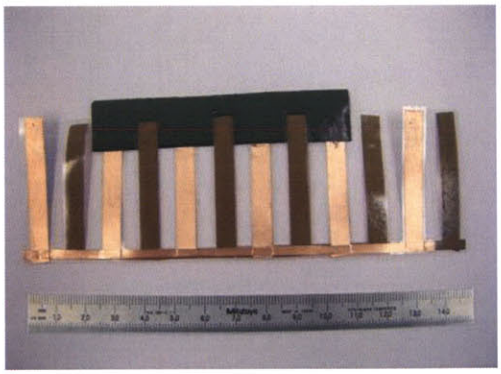

(b) Comb style flexure.

Figure 6-4: Flexural supports used to constrain trilayer deflection.

6.1.2 Mechanical Structures

Bryan Schmid discusses methods to control directions of deflection in his thesis, [31]. The three deflection governing options were geometry manipulation, internal shim placement, and external mechanical restraints. An example of geometry manipulation is cutting trilayers in a way to maximize the length to width ratio. Since the polypyrrole contracts uniformly in every direction, its preferential direction of curl will be along its major axis.

Several successful attempts were made to create external mechanical constraints for trilayers. Flexural structures were laser cut out of plastic transparency sheets to provide the trilayers with structural stiffness, which allowed trilayers to bend easily in one direction but not in others. Copper tape with conductive adhesive was used to provide regularly spaced points of electrical contact along the trilayer.

In an effort to move towards a biologically-inspired fin, Figure 6-5(a) shows a support flexure cut to resemble a fin with copper patterns for electrical contacts. Figure6-5(b) is the same fin with conducting polymer trilayers incorporated. Cupping motion was achieved in this fin. However, the strain rate was relatively low compared to normal trilayer actuation. The slow strain rate could be attributed to the high stiffness of the plastic support structure. Further iterations of this flexural fin should be designed to reduce the stiffness of the flexure along the direction of cupping.

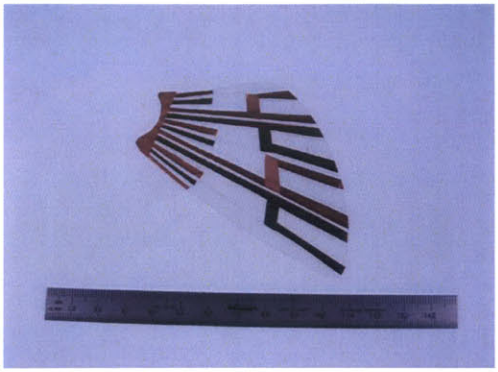

(a) Flexure cut to resemble the pectoral fin of a fish.

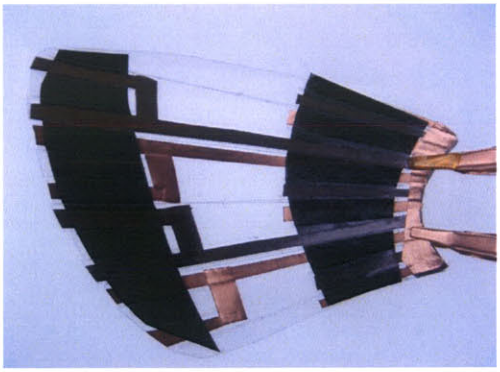

(b) Conducting polymer trilayers integrated into the fin.

Figure 6-5: Conducting polymer actuated fin.

6.2 Underwater Actuation

In order for trilayer technology to useful in AUV applications, the actuators must be able to actuate in water. Simple tests were done to show that the trilayers could exert enough force to achieve sweeping motions underwater. A polyethylene sleeve was made to encapsulate the segment of trilayer submerged in the water to prevent delamination of the trilayer. Figure 6-6 shows the actuation of an encapsulated trilayer in water. It is able to complete 2 full sweeps in 5 seconds. Vortical flow was apparent with the addition of green dye.

This simple test in conjuction with the force data presented in Chapter 5 proves that trilayers have the capability of actuating in water. However, in this particular test, the polyethylene sleeve was too stiff to allow for any curvature along the length of the trilayer. Also, the point of electrical contact is still above water.

6.2.1 Encapsulation

Steps were taken to encapsulate the trilayer and the electrical contacts so that the entire package could be submerged in water. Different methods of encapsulation were explored. Trilayers were laminated between thin sheets of mylar 6 μm thick (Figure 6-7. Spray adhesive was used as the means of holding the package together. This

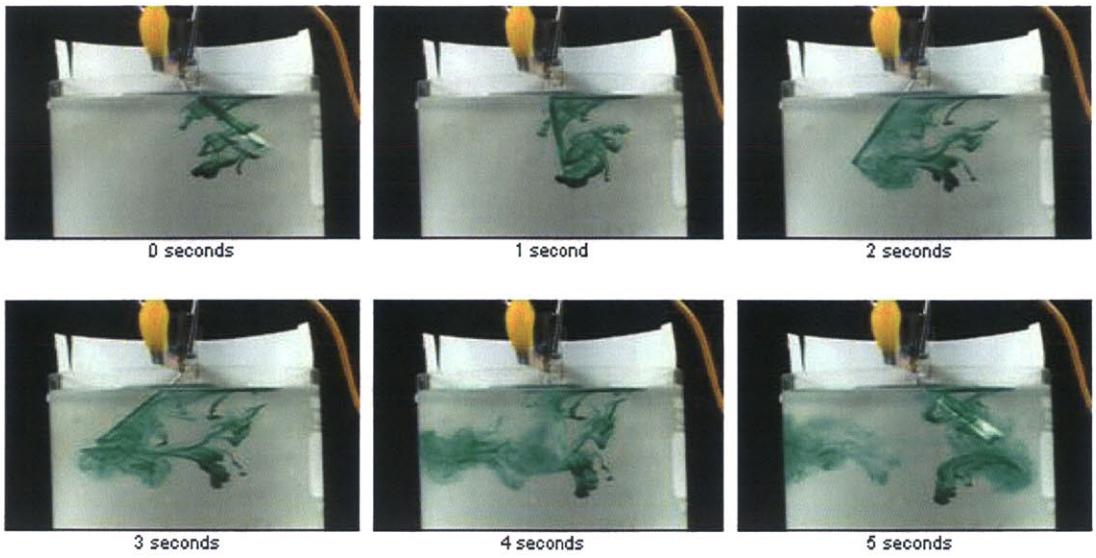

Figure 6-6: Actuation of an encapsulated trilayer underwater over a 5 second period. Two full sweeps are captured.

method succeeded in protected the trilayers from the outside elements. However, the spray adhesive greatly impeded the motion of the trilayer.

Another method of encapsulation was explored with a pressure sensitive plastic sealing wrap. The surface of the plastic has many bumps and ridges. A light adhesive developed by Procter and Gamble called Griptex is strategically placed only in the ridges. Therefore, the plastic only adheres when its ridges have been pressed down to touch a surface. This method worked well as the trilayer was not impeded as much by the light adhesive.

One problem that does tend to occurs however is melting of the encapsulation material near the electrical contacts due to over heating. However, this can be avoiding by using the duty cycle actuation scheme described in Chapter 5 or by developing a more sophisticated feedback control loop to control the temperature distribution in the trilayer.

6.2.2 Alternatives

Since trilayer actuators would eventually be used in water as a means of maneuvering and propulsion, it is conceivable that the electrolyte gel, currently used as the source

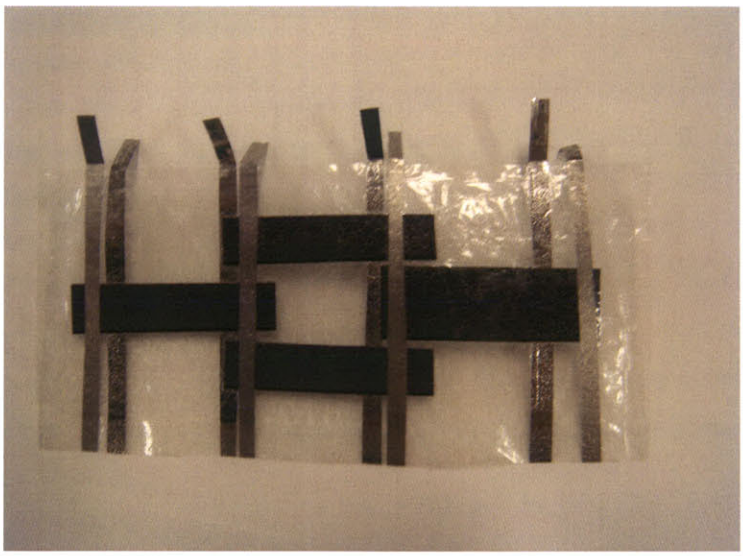

Figure 6-7: Trilayers laminated with mylar and spray adhesive.

of ions as well as a means of adhesion, could be completely eliminated. Instead, the trilayer could use salt water as an ion source. A trilayer-like actuator was quickly assembled using porous gauze material sandwiched between two polymer strips and held together with spray adhesive. Once lowered into water, the gauze trilayer was actuated like a regular trilayer. Since the ions from the salt water were different from the ions in the $BMIMBF_4$, the direction of curvature was actually in the opposite direction from the normal trilayers.

Chapter 7

Summary

Power supplied to actuate trilayers is converted either to mechanical work or is lost through resistive joule heating. At low currents, most of the power is converted to mechanical work as the polypyrrole layers expand and contract and minimal heating occurs. At high voltages and current, heating can be observed. The heating profile of the trilayers can be affected by spacing of electrical contacts, magnitude of input voltages, and signal frequency. This heating effect can be exploited to improve actuator strain rates.

From experimental results, it has been shown that temperature has an effect on mechanical, electrical, and electrochemical properties of the polypyrrole film and electrolyte gel. The modulus of both the gel and the film decrease as temperature increases reducing the flexural rigidity of the trilayer which may partially explain the increase in performance of a trilayer during repeated actuation cycles. The other factor that improves performance is the admittance of the electrolyte gel. Increases in temperature improve ion mobility, which in turn improves strain rate.

The impedance of a trilayer plays an important role in determining it effectiveness as actuator. High performance trilayers tend to have a low impedance on the order of 300 Ohms at room temperature and can decrease even more with actuation. Repeated actuation cycles at high voltages has a compounding effect on the strain rate of a trilayer. However driving trilayers with large voltages runs the risk of overheating and degrading the polymer. Trilayers can be induced into a state of lower impedance

with high frequency pulses of high voltages at low duty cycles. This method is a more efficient way of actuation because less energy is lost through resistive overheating. Trilayers exhibit very good performance at temperatures around 325 K generating forces up to 40 mN and force rates up to 25 mNs^{-1} for a 10 mm by 10 mm section. These values give an idea of the amount of thrust that could be produced if trilayers were used as a means of propulsion in an underwater environment.

Initial steps have been taken to use the knowledge gained from the temperature experiments to integrate trilayers into actively controlled hydrodynamic surfaces and achieve the necessary strain rates and forces required for underwater propulsion and maneuvering. There is much room for future work in this particular application.

Bibliography

[1] Standard practice for plastics: Dynamic mechanical properties: Determination and report of procedures. ASTM Standard: D 4065-01.

[2] P. Anquetil. *Large Contraction Conducting Polymer Molecular Actuators.* PhD thesis, Massachusetts Institute of Technology, 2004.

[3] P. Bandyopadhyay. Trends in biorobotic autonomous undersea vehicles. *IEEE Journal of Oceanic Engineering*, 30:109 – 139, 2005.

[4] Y. Bar-Cohen, editor. *Electroactive Polymer (EAP) Actuators as Artificial Muscles: Reality, Potential, and Challenges.* SPIE Press, 2001.

[5] R. Baughman, R. Shacklette, and R. Elsenbaumer. Microelectromechanical actuators based on conducting polymers. *Molecular Electronics*, pages 267–89, 1991.

[6] L. Bay, K. West, P. Sommer-Larsen, S. Skaarup, and M. Benslimane. A conducting polymer artificial muscle with 12*ADVANCED MATERIALS*, 15(4):310–313, February 2003.

[7] S.N. Davidson. Development of conducting polymer based biomimetic muscles and fabrication techniques for and artificial pectoral fish fin. Master's thesis, Massachusetts Institute of Technology, 2005.

[8] M. Del Zio. Thermal effects on polypyrrole actuation. Master's thesis, Massachusetts Institute of Technology, 2006.

[9] A. DellaSanta, A. Mazzoldi, and D. DeRossi. Steerable microcatheters actuated by embedded conducting polymer structures. *JOURNAL OF INTELLIGENT MATERIAL SYSTEMS AND STRUCTURES*, 7(3):292–300, May 1996.

[10] F Gray. *Solid Polymer Electrolytes.* VCH Publishers, Inc, 1991.

[11] S. Hara, T. Zama, W. Takashima, and K. Kaneto. Tfsi-doped polypyrrole actuator with 26% strain. *Journal of Materials Chemistry*, 14:1516–1517, 2004.

[12] IW Hunter and S. Lafontaine. A comparison of muscle with artificial actuators. *Solid-State Sensor and Actuator Workshop, 1992. 5th Technical Digest., IEEE*, pages 178–185, 1992.

[13] E. W. H. Jager, E. Smela, O. Inganas, and I. Lundstrom. Polypyrrole microactuators. *SYNTHETIC METALS*, 102(1-3):1309–1310, June 1999.

[14] G. V. Lauder, P. Madden, R. Mittal, H. Dong, M. Bozkurtas, N. Davidson, J. Tangorra, and I. Hunter. Pectoral fin function in sunfish: Experimental hydrodynamics, computational fluid dynamics, and construction of a robotic model. *INTEGRATIVE AND COMPARATIVE BIOLOGY*, 45(6):1030–1030, December 2005.

[15] S.K. Lee, S.J. Lee, H.J. An, S.E. Cha, J.K. Chang, B. Kim, and J.J. Pak. Biomedical applications of electroactive polymers and shape memory alloys. *Proceedings of SPIE, the International Society for Optical EngineeringProceedings of SPIE, the International Society for Optical Engineering*, 4695:17–31, 2002.

[16] WH Li, G.M. Spinks, LB Zhao, YZ Wu, D. Zhou, and G.G. Wallace. Characterization of conducting-polymer-based bimorph vibration sensors. *Proceedings of SPIE*, 5648:301, 2005.

[17] J. Madden. *Conducting Polymer Actuators.* PhD thesis, Massachusetts Institute of Technology, 2000.

[18] J. Madden, I. W. Hunter, and R. J. Gilbert. Development of an artificial muscle fiber composed of the conducting polymer actuator polypyrrole. *GASTROENTEROLOGY*, 122(4):A164–A164, April 2002.

[19] J. Madden, P. Madden, and I Hunter. Conducting polymer actuators as engineering materials. In *Proceedings of SPIE*, volume 4695, 2002.

[20] J. D. Madden, R. A. Cush, T. S. Kanigan, and I. W. Hunter. Fast contracting polypyrrole actuators. *SYNTHETIC METALS*, 113(1-2):185–192, June 2000.

[21] J. D. W. Madden, B. Schmid, M. Hechinger, S. R. Lafontaine, P. G. A. Madden, F. S. Hover, R. Kimball, and I. W. Hunter. Application of polypyrrole actuators: Feasibility of variable camber foils. *IEEE JOURNAL OF OCEANIC ENGINEERING*, 29(3):738–749, July 2004.

[22] J. D. W. Madden, N. A. Vandesteeg, P. A. Anquetil, P. G. A. Madden, A. Takshi, R. Z. Pytel, S. R. Lafontaine, P. A. Wieringa, and I. W. Hunter. Artificial muscle technology: Physical principles and naval prospects. *IEEE JOURNAL OF OCEANIC ENGINEERING*, 29(3):706–728, July 2004.

[23] P. Madden. *Development and Modeling of Conducting Polymer Actuators and the Fabrication of a Conducting Polymer Based Feedback Loop.* PhD thesis, Massachusetts Institute of Technology, 2003.

[24] P. Madden, J. Madden, P. Anqetil, H. Yu, T. Swager, and I. Hunter. Conducting polymers as building blocks for biomimetic systems. In *Proceedings of the 12th International Symposium on Unmanned Untethered Submersible Technology*, 2002.

[25] L. Masaro and XX Zhu. Physical models of diffusion for polymer solutions, gels and solids. *Prog. Polym. Sci*, 24:731–775, 1999.

[26] T. F. Otero and M. T. Cortes. Artificial muscle: movement and position control. *Synth. Met*, 102(3):1317, February 1999.

[27] T.F. Otero and M.T. Cortes. Characterization of triple layers. *Proceedings of SPIE*, 4329:93, 2003.

[28] Q. B. PEI and O. INGANAS. Electrochemical applications of the bending beam method .1. mass-transport and volume changes in polypyrrole during redox. *JOURNAL OF PHYSICAL CHEMISTRY*, 96(25):10507–10514, December 1992.

[29] R. Pytel, E. Thomas, and I. Hunter. Anisotropy of electroactive strain in highly stretched polypyrrole actuators. *CHEMISTRY OF MATERIALS*, 18(4):861–863, February 2006.

[30] S Roth. *One-dimensional Metals.* Springer-Verlag, 1995.

[31] B Schmid. Device design and mechanical modeling of conducting polymer actuators. Bachelor's Thesis, 2003.

[32] S. Sherrit and Y Bar-Cohen. *Electroactive Polymer (EAP) Actuators as Artificial Muscles: Reality, Potential, and Challenges*, chapter Methods of Testing and Characterization, pages 405–453. SPIE Press, 2001.

[33] E. Smela. Microfabrication of ppy microactuators and other conjugated polymer devices. *JOURNAL OF MICROMECHANICS AND MICROENGINEERING*, 9(1):1–18, March 1999.

[34] E. Smela. Conjugated polymer actuators for biomedical applications. *ADVANCED MATERIALS*, 15(6):481–494, March 2003.